Probing the role of anchoring ligands in charge separation dynamics of novel zinc-phthalocyanine sensitized TiO_2 films through ultrafast spectroscopy

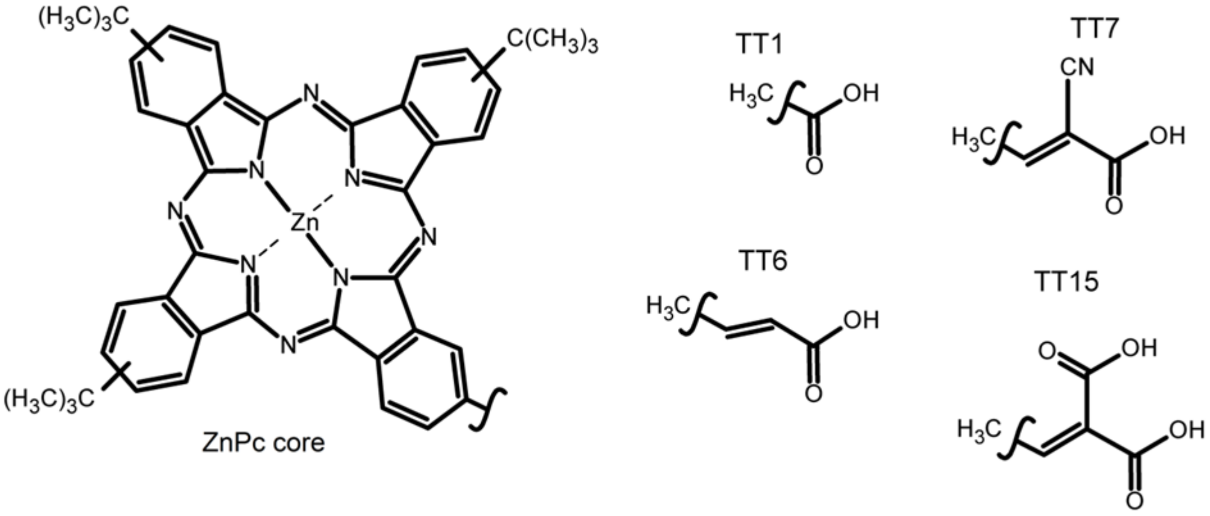

Gerwin Steen

MSc thesis Applied Physics

8 March 2013

University of Twente

Probing the role of anchoring ligands in charge separation dynamics of novel zinc-phthalocyanine sensitized TiO_2 films through ultrafast spectroscopy

G.W. Steen
March 2013

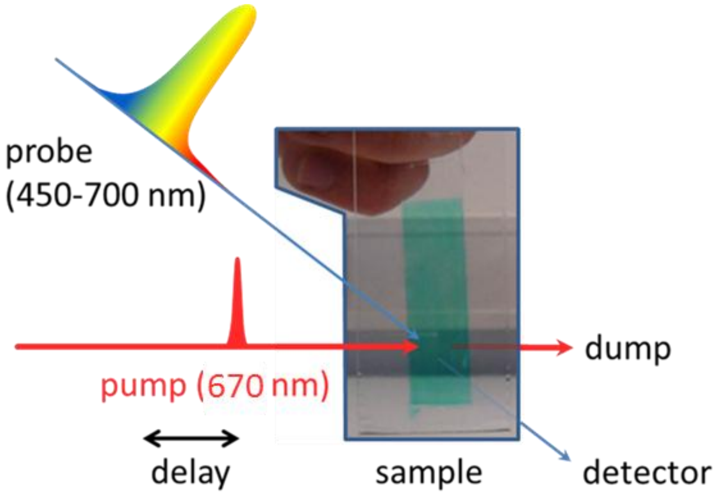

A master thesis presented to the faculty of University of Twente in partial fulfilment of the requirements for the degree of Master of Science

Graduation Committee

Prof. Dr. J.L. Herek, Optical Sciences, University of Twente
Dr. Ir. A. Huijser, Optical Sciences, University of Twente
Dr. D. Sharma, Optical Sciences, University of Twente
Dr. C. Blum, Nanobiophysics, University of Twente

University of Twente
Enschede - The Netherlands

Optical Sciences

Faculty of Sciences & Technology
University of Twente
Enschede, The Netherlands

Summary

This master project is focused on zinc-phthalocyanine (ZnPc), a molecule absorbing in the red range of our solar spectrum. The high photon flux in this region makes the dye interesting to use in dye sensitized solar cells (DSSCs). Such solar cells are based on dye molecules that are adsorbed onto a highly porous nanocrystalline semiconductor, usually TiO_2. After absorbing sunlight, the excited dye injects one electron into the TiO_2 (the anode) conduction band on an ultrafast timescale. The electron diffuses through the anode after which it is being collected at one of the electrodes. From the electrode it travels through a load and is recollected by the platinum film (the cathode). The electron finally enters a liquid conductor that resupplies the dye with its missing electron. Recent research has shown that process rates of electron injection (EI) and electron recombination greatly influence the performance of DSSCs. By modifying the anchoring ligand these processes rates can be controlled. In this work the dynamics of charge separation of four different anchoring ligands designs for ZnPc have been characterised by a femtosecond transient absorption setup.

Acknowledgements

I would like to express my very great appreciation to Dr. Annemarie Huijser and Dr. Divya Sharma, my project supervisors, for their useful critiques, guidance and encouragement and given advice. It has been a great help in finding a suitable AIO position. I would also like to thank Prof. Jennifer Herek for the enthusiasm with which she leads the weekly group meeting, which gave me good opportunities to feel connected and discuss my project with other members of the Optical Sciences group. For these discussions I want to thank Dan Chen, Dirk Jan Dikken, Andrew Fussell, Erik Garbacik, Rick Krabbendam, Jorick van ‘t Oever, Qing Pan, Amendev Singh, Frank Timmermans, Bente Elschot and Tomas Huisman.

I want to thank Florian Sterl for showing me some new tricks with ‘Matlab’, Simon Huisman for borrowing the silica power detector and Sun-Young whom I could give a short introduction to the transient absorption setup and thus experience how to present the setup.

I would like to thank Ing. Jeroen Korterik for the technical support he gave me during the building of the dynamics sample holder and the maintenance he provided for the transient absorption setup. I am thankful for Ing. Frans Segerink my go-to person when I needed chemicals and other necessary materials. I wish to acknowledge Karen Munnink for supplying me with necessary office materials.

I would like to extend my thanks to Prof. Dr. Jurriaan Huskens of the molecular nanofabrication (MNF) group for letting me use their ‘PerkinElmer’ fluorescence spectrometer and to Ing. Richard J.M. Egberink for introducing me to the fluorescence spectrometer.

I am thankful for the RSK ‘kringgroep’ for showing interest in my work.

Finally, I wish to thank my parents for never stopping supporting me.

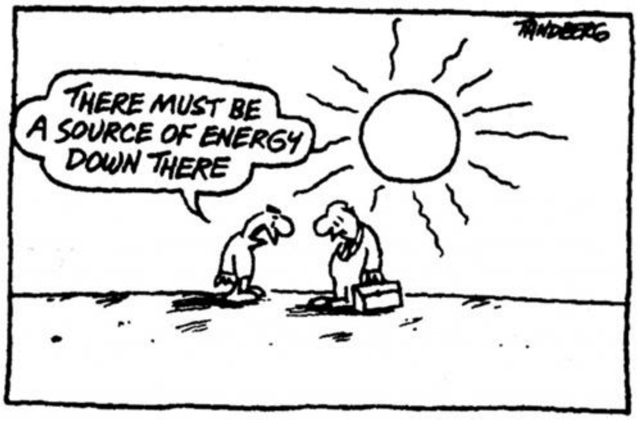

Reference: [28]

Table of Contents

1. Introduction

The use of fossil fuels to meet our energy consumption is polluting our planet and we can expect these sources to deplete. Understanding how to optimise the energy harvesting of clean renewable energy sources is necessary to meet our ever growing demand for energy. A great and practically unlimited source of clean energy is our sun. The total irradiance of sunlight at the top of the atmosphere is according to measurements from the total irradiance monitor (TIM) 1360.8 ± 0.5 Wm^{-2} during the 2008 solar minimum period.[14] According to ASTM E 892 standard the total (integrated over all wavelengths) global irradiance of sunlight going through an air mass (AM) of 1.5 is 963.8 Wm^{-2} on a horizontal surface at ground level.[27] Most solar cells only have a certain range in which they are able to operate as shown in Figure 1.1. Other than directly transformation into electrical energy, sunlight can also be converted into thermal energy or used to produce hydrogen.

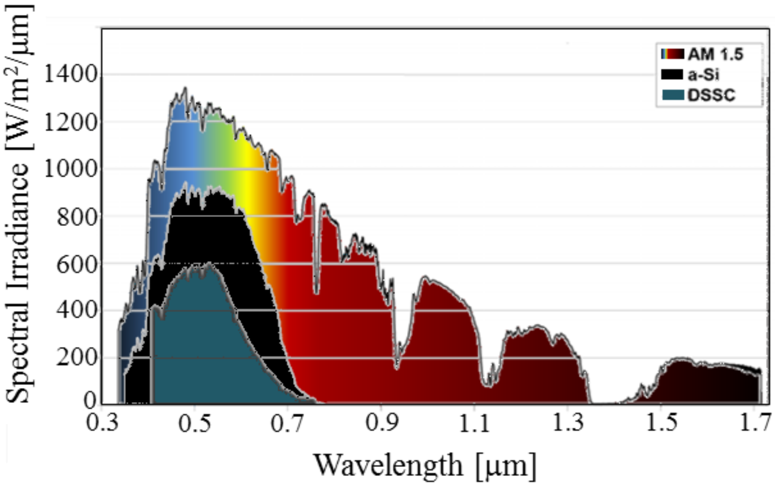

Figure 1.1 – AM1.5 global solar spectrum plotted with the response of double junction amorphous silicon solar and a DSSC.[12]

In order to make more efficient conversion devices, first the fundamental processes need to be fully understood. For photovoltaic conversion these processes are: light absorption, excited state thermalisation, energy diffusion, charge separation, charge transport and charge collection.[15]

Commercial solar cells widely used multi crystalline silicon. Their efficiencies have been measured as high as 20.4 ± 0.5% under global AM1.5 spectrum. The record of 44.0 ± 3% was achieved by multijunction cells of InGaP/GaAs/InGaAs.[17] However these world record solar cells are not commercially attractive, since they consist of expensive rare earth elements. For production of these solar cells one also needs to take into account the amount of energy it requires to produce the product: roughly five year of energy harvesting of a silicon based solar is needed to make enough silicon out of silicon oxide. This is due to the fact that very pure, and thus expensive, silicon is needed. Another disadvantage of silicon based solar cells is the temperature effect upon the efficiency of the solar cell.[16]

Promising replacements of silicon based solar cells are dye sensitized solar cells (DSSCs). The first prototypes were already made 22 years ago by their inventor Prof. Michael Grätzel and co-workers.[16] Unlike silicon based materials, these DSSCs have a wide temperature range in which they are able to convert sunlight into usable energy and are able to work under lower intensities of light. Dyes used for the absorption of light are much cheaper to use and much optimisation is still possible. The complete DSSCs are relative cheap to produce compare to silicon solar cells and mechanically much easier to work with. However the major problems for worldwide production of DSSCs are the cathode, which is made of the expensive material platinum and the iodine based electrolyte, which is extremely corrosive. However studies are being done to avoid using this electrolyte.[20] Many research groups are involved in increasing the efficiency of DSSCs. [19] It has been shown that the efficiency of DSSCs depends on the interfacial processes of the dye-semiconductor.

1.1 Dye sensitized solar cells

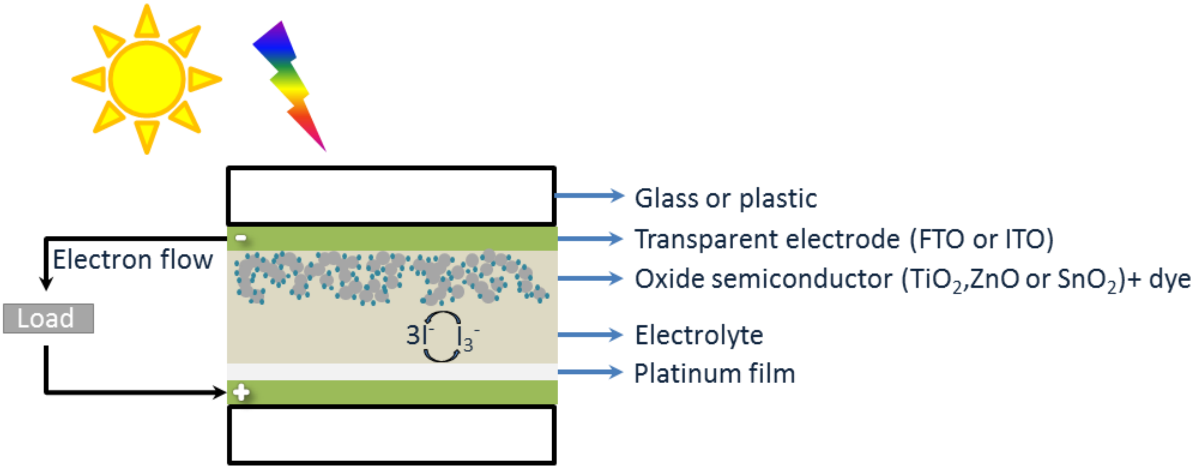

Figure 1.2 – Design of a dye sensitized solar cell: A electrode of (grey dots) nano porous oxide semiconductor film on top of a (green) fluorine-doped tin oxide (FTO) or indium tin oxide (ITO) coated glass substrate responsible for electron transport, (than) a redox electrolyte, most commonly used redox couple is iodide/triiodide, (blue) dye responsible for light absorption and a counter electrode of a transparent electrode coated with a (silver) platinum film.

A dye sensitized solar cell (DSSC) consists usually of the following elements: [22]

- Two transparent electrodes usually made out of fluorine-doped tin oxide (FTO). The counter electrode, commonly platinum-coated FTO, exhibit high catalytic activity for electron transfer to the redox electrolyte.
- A redox electrolyte, commonly used redox coupled is iodide / triiodide, to regenerate the oxidized dye.
- A highly porous nano crystalline oxide semiconductor (anode) usually made of TiO_2 nanoparticles.
- A molecular dye able to absorb sunlight.
- Two insulating and transparent substrates (glass or plastic).

Excitons are formed when sunlight is absorbed by the dye. This light needs to pass through the cathode and the liquid conductor. The excited dye injects an electron into the semiconductor. Two different electron injection (EI) rates into a semiconductor are usually observed. The time windows in which these processes take place are ranging from less than 100 fs to tens of ps.[26]

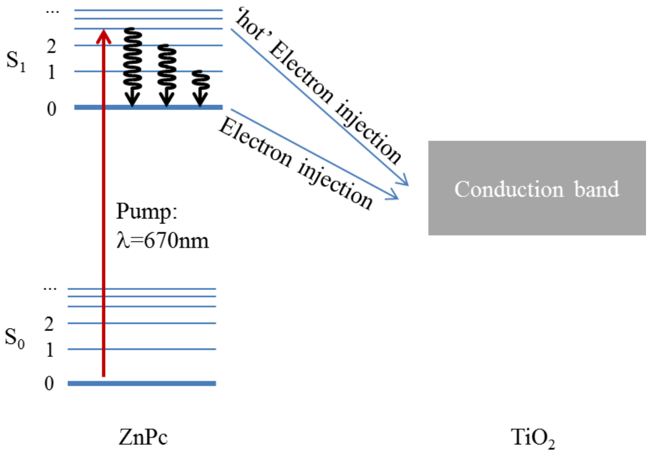

Figure 1.3 – Explanation of bi exponential kinetics: The pump does not necessarily excite the first electronic level of the first excitation band. The extra energy is quite quickly (femtoseconds range) dissipated into vibrational energy (basely heat), indicated by the black arrows.[19]

The rate of 'hot' electrons injection is in the fs region, while the injection rate of the relaxed excited electron is in the ps region or even slower. EI from an excited dye can be prevented by exploiting a material with a lowest unoccupied molecular orbit (LUMO) energy level higher than the excited state of the dye, such a material is Al_2O_3.

To achieve high efficiency of a dye in a DSSC a large spectral overlap with the solar emission spectrum is required. Also a fast EI into the conduction band of the semiconductor and a slow charge recombination between the injected electron and the dye cation is essential.[6]

Using ruthenium dye, efficiencies of up to 11% have been obtained in TiO_2-based DSSCs.[7] However they have limited availability and are unable to absorb light with wavelengths around 700 nm.

1.2 Zinc-phthalocyanine

Phthalocyanines are attractive molecules due to their high (>100000 $dm^3 \cdot M^{-1} \cdot cm^{-1}$) molecular extinction coefficients in the red/IR red region of the solar spectrum. This region of the solar spectrum exhibit high photon flux. Zinc-phthalocyanine (ZnPc) has strong tendency to aggregate on TiO_2, this and the lack of directionality in the electron transfer process towards the semiconductor results in low (< 1%) efficiencies in DSSCs.[13] Reducing the aggregation onto the semiconductor film was predominantly achieved by the design of peripheral substituents on the phthalocyanine ring. The use of chenodeoxycholic acid (cheno) also reduces the formation of aggregates. By a high perturbed electronic structure of the molecules also high injection rates are expected. This can be achieved through designing anchoring ligands which have strong covalent bond with the TiO_2 film.[4] Leading to: higher surface coverage, increased stability, minimal desorption, monolayer coverage and increased strength of the electronic coupling between the molecular orbital of the dye and the semiconductor levels, which leads to fast injection rates[9].

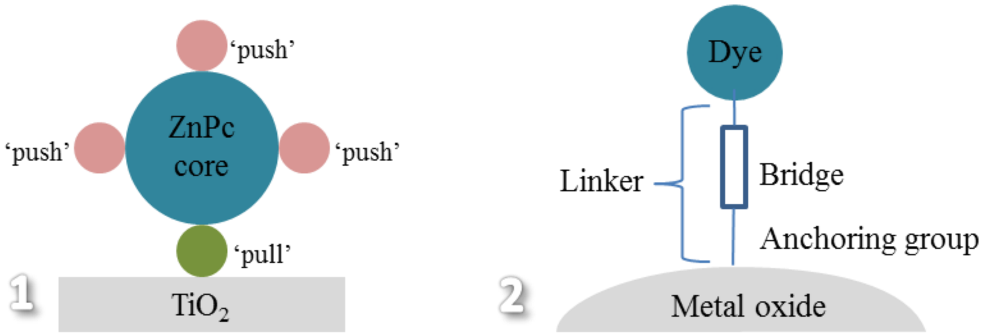

Figure 1.4 – Two schematic representations of unsymmetrical ZnPc anchored on TiO_2, (2) dye bound to metal oxide nanoparticle surface by a general linker.

Figure 1.5 shows the design of four novel ZnPcs: the dye contains three tertbutyl groups that act as 'push' group to minimize the aggregation, enhance the solubility and tune the energy level of the LUMO to provide directionality in the excited state. The different anchoring groups act as 'pull' groups.[1][5][8] The molar mass of TT1, TT6, TT7 and TT15 are respectively 796.288 $g \cdot mol^{-1}$, 822.324 $g \cdot mol^{-1}$, 847.32 $g \cdot mol^{-1}$ and 866.334 $g \cdot mol^{-1}$.

The design of the linker can influence the electron injection (EI) and recombination rates.[10][11] TT1 and TT6 based DSSCs have efficiencies of 3.5% and 3.28, much higher than the ZnPc without linker based DSSCs could achieve. The only difference between TT1 and TT6 is the bridge, creating more distance between the donor and acceptor. TT15 based DSSCs gave an even better efficiencies of 3.96%. TT15 has an extra COOH group, which can force a different orientation of the molecule. TT7 based DSSCs only gave an efficiency of 2.55. The TT7 molecule has a CN group, which was expected to increase the electron transfer rate in both directional: both EI and recombination. Perhaps the recombination rate is faster than the EI rate.[1]

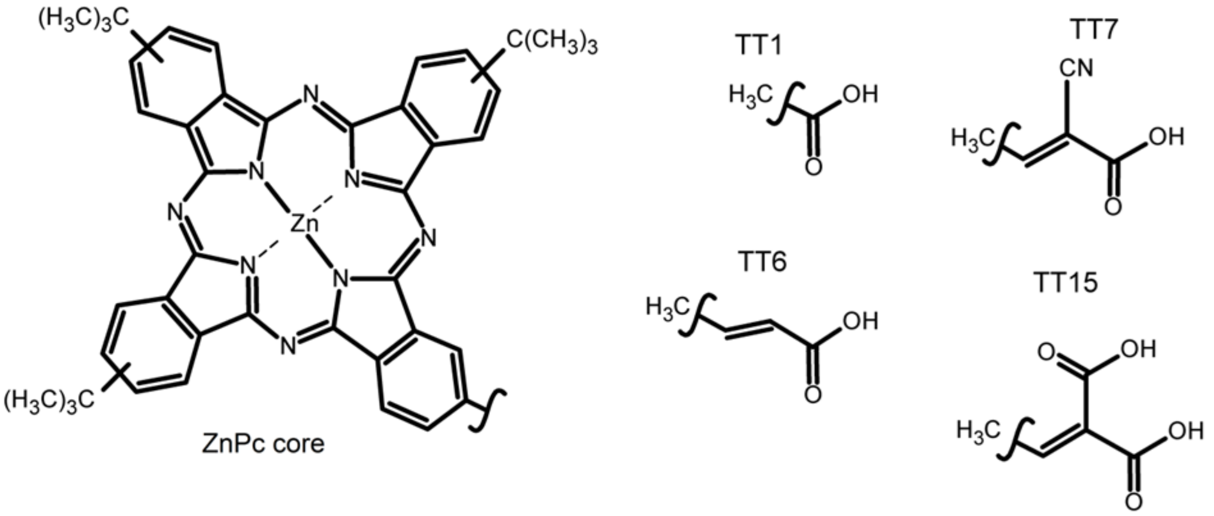

Figure 1.5 – Molecular structure of (left) Zinc-Phthalocyanine, with its (right) different anchoring ligands.

1.3 Electron transfer

Electron transfer includes both the forward electron transfer (electron injection) and the backwards electron transfer (recombination). The rate of electron transfer from a donor to an acceptor depends on four parameters, as given in the simplest form of Markus theory, see Equation 1.1. This equation is valid for electron transfer within the non-adiabatic (weak D/A coupling) transition-state.

$$\mathrm{k}_{ET} = \sqrt{\frac{\pi}{\hbar^2 \lambda k_B T}} V_{DA}^2 exp\left(-\frac{(\Delta G^0 + \lambda)^2}{4\lambda k_B T}\right)$$

Equation 1.1

Where: λ is the reorganization energy (also called vibronic coupling energy): the amount of free energy needed to move along the nuclear coordinate of the donor indicated by A in Figure 1.6, to the position above the minimum of the acceptor as indicated by B in Figure 1.6, ΔG^0 is the change in Gibbs free energy between the relaxed acceptor state and the relaxed donor state, V_{DA} is the electronic coupling and T is the temperature.[18]

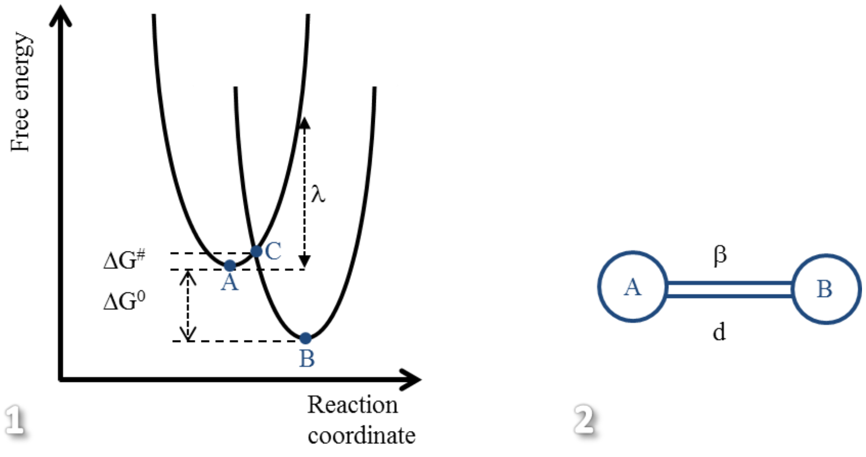

Figure 1.6 – Schematic representation of the parameters vital for calculation the electron injection rate.

TT1, TT6, TT7 and TT15 have similar electrochemical properties,[1] however modifications of the linker can lead to different orbital overlap and thus different electronic coupling. The expected electronic coupling V between a distance of d between centre donor to centre acceptor depends on the coupling V_0 at a centre donor to centre acceptor distance of d_0 as can be seen in Equation 1.2, where β a damping factor is, which depends on the medium between donor and acceptor. For example: a lower electronic coupling is expected for TT6 when compared to TT1.[18]

$$V = \mathrm{V}_0 \, exp\left(-\frac{\beta}{2(d-d_0)}\right)$$ **Equation 1.2**

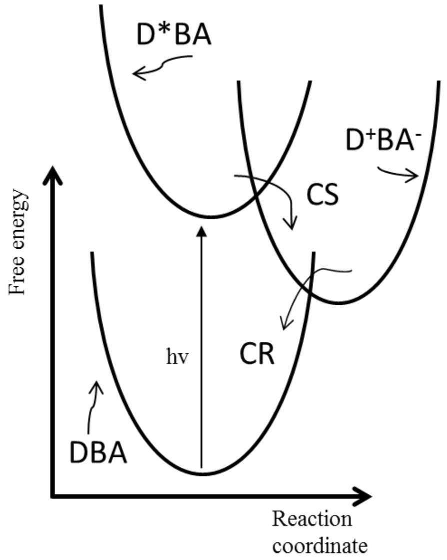

Figure 1.7 – Schematic representation of photo initiated electron transfer charge separation (CS) after absorption of a photon, followed by charge recombination (CR) to the ground state. D stands for donor, B for bridge and A for acceptor.

1.4 Aim of work

By further improving the anchoring ligand, even higher efficiencies might be reached. Therefore the impact of anchoring ligand on electron transfer and recombination dynamics needs to be identified. This characterisation has been done by time-resolved pump-probe spectroscopy. For this project the non-collinear optical parametric amplifier (NOPA) was tuned to a centre excitation wavelength of 670 nm to excite the novel ZnPc molecules. A dynamic sample holder has been designed and made to prevent sample degradation and accumulation of long-living states. Compression of pump pulses is achieved by a prisms set to produce near Fourier transform limited (TL) pulses. Thus minimize the chirp of the pump and producing the shortest possible pulses, which was verified by correlation technics. A second harmonic generation (SGH) autocorrelation and an SHG-frequency-resolved optical gating (FROG) setup have been built. Alongside the optimization of the transient setup, also the preparation of the samples has been optimized. The ZnPc with its different anchoring ligands have been synthesised by Prof. Torres and co-workers of the University of Madrid. When measuring we ensured a 54.7 degrees difference between pump and probe polarization to prevent anisotropy effects. The possibility that a reference beam might improve the setup, has been checked, but has proven to be unnecessary. Luminescence measurements on TT1, TT6, TT7 and TT15 in solution have been performed to be able to explain the transient data.

The main goal of this work has been to successfully describe the impact of different anchoring ligands on electron transfer: the electron injection into the conduction band of a semiconductor and the recombination. This knowledge is helpful in understanding the observed differences in efficiencies of the novel ZnPc and will help to optimize the linker.

1.5 Thesis overview

The thesis is constructed as followed:

- The second chapter of this thesis provides theory regarding transient absorption spectroscopy (TAS).
- The third chapter describes the transient absorption setup and provides technical information.
- The fourth chapter describes the preparation steps to make samples of ZnPc anchored onto TiO_2 films.
- The fifth chapter presents the achieved results and includes a discussion.
- Concluding words and recommendations can be found in the sixth chapter.

- The final chapter contains a summary list of the used abbreviations with their full names.

2. Theoretical framework

This chapter discusses the theoretical background of transient absorption spectroscopy. First the more familiar linear absorption is discussed. The next paragraph describes transient absorption. The last paragraph describes the principles of a second harmonic generation $^{(SHG)}$-autocorrelator, which is commonly used to quantize the time duration of an optical ultra-short pulse.

2.1 Transient absorption spectroscopy

2.1.1 Linear absorption

Linear absorption spectrum gives information how strongly light is absorbed for each wavelength. For light to be absorbed, it has to match the available energy states in the atoms or molecules. The probability that light is absorbed or scattered by an atom or molecule is related to the cross section σ. Its value can be smaller or larger than the geometric cross section. Lambert-Beer law describes for the macroscopically world the relation between linear absorption and scattering of light and the medium through with the light is passing. This relationship is described in Equation 2.2,

$$I = I_0\, exp(-\sigma Cl) = I_0\, exp(-\mu l)$$

Equation 2.1

where I is the intensity transmitted through the sample and I_0 is the reference intensity transmitted without a sample. The molar absorption coefficient ε is defined as log(e) times the cross section, C is the concentration of molecules in the sample and l is the thickness of the sample. The quantity absorption $^{(A)}$, also called optical density $^{(OD)}$ is defined as:

$$\mathrm{A} = OD = -log10\left(\frac{I(\lambda)}{I_0(\lambda)}\right) = -log10\left(\frac{I(\lambda)\exp(-\sigma Cl)}{I_0(\lambda)}\right) = \varepsilon l C$$

Equation 2.2

To be able to characterize the dynamics of the excited state, one needs to be able to probe at time scales at which these processes are happening.

2.1.2 Transient absorption

This can be done with a transient absorption measurement. Just like a linear absorption measurement the transmission of a white light continuum $^{(WLC)}$ source is measured. However instead of a continuous source a pulse probe is used. Another major difference is the use of a pump beam: the transmission of probe pulses is measured after excitation of the molecules and in case the pump pulses are absent at different delay times between both pulses. The resolution of a transient absorption measurement is limited by the time duration of these pulses.

The delta optical density (ΔOD) measured with a transient absorption setup is given as the minus log 10 of the intensity measured with pump at a certain time delay divided by the intensity measured in case pump pulses are absent, see Equation 2.3. If the probe pulses arrive before the sample is pumped, a zero line is expected, because the ratio of the absorption spectra will be one. The same is true in case pump pulses are absent.

$$\Delta OD = -log10\left(\frac{I(\omega,\Delta\tau)_{Pumped}}{I(\omega)_{Not\ pumped}}\right) \qquad \textbf{Equation 2.3}$$

To be able to measure the ΔOD signal, halve of the pump pulses need to be cut off. This is achieved by modulating the pump beam by a chopper. To ensure a certain delay between pump and probe pulse, the optical path of the probe pulses are controlled by a delay state. The pump beam and probe beam are focused onto a sample and are spatially overlapped. The pump beam is blocked after passing through the sample.

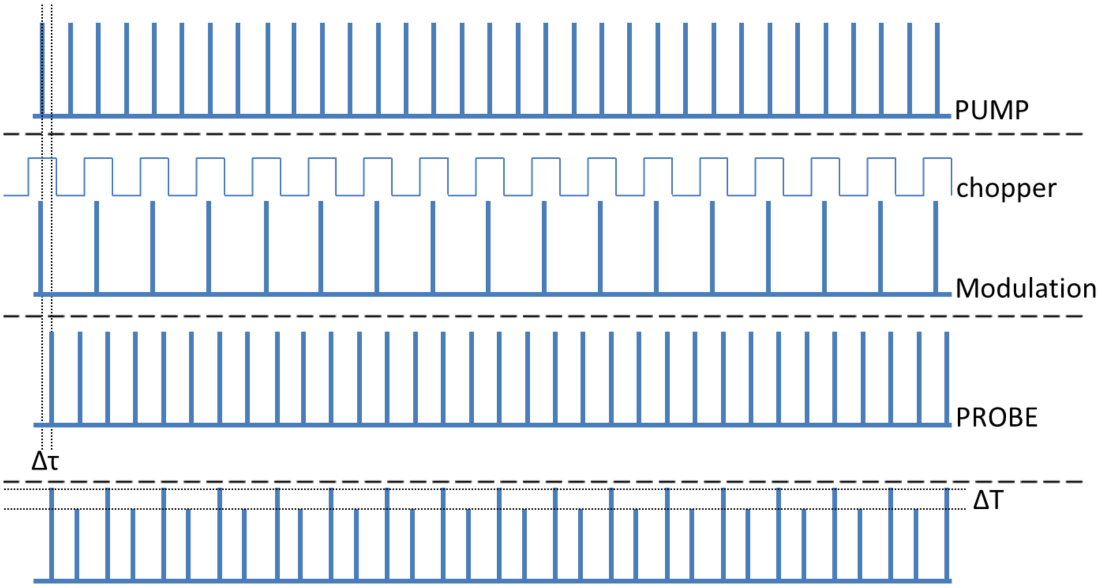

Figure 2.1 – Explanation of calculated delta absorption spectrum: The pump beam is modulated by a chopper. The probe pulses are delayed by a delay line, to be able to measure the system at certain time after being excited.[15]

The probe beam is sent into a spectrometer, where a charged coupled device (CCD) is measuring the intensity of the probe pulses. The input from the chopper is used to distinguish between the signals from a pumped sample and the signals in absent of the pump. The time delay stage is controlled to observe the signal at different time delays between pump and probe pulses. The delta absorption spectrum is extracted from a pump probe experiment. Generally a subtraction is made for the background light. The intensity needs to be limited in order to prevent non-linear processes and degradation of the sample. A delta optical density spectrum contains a contribution from various processes namely:

- Ground state bleach (GSB): The pump beam excites the sample from the ground state, thus the probe beam sees less number of molecules in the ground state. Therefore the ground state absorption is less than for a sample that has not been excited. A higher transmitted signal corresponds to a negative delta absorption signal.
- Stimulated emission: is Stokes shifted with respect to the ground state bleach. The light intensity on the CCD camera has increased due to stimulated emission, therefore a negative signal is observed.
- Spontaneous emission: even in absence of the probe light an excited state will eventual undergo a transition to a lower energy state. The lifetime depends on the properties of the molecule and the mode structure of the surrounding medium.
- Excited state absorption (ESA): higher excited states transition might exist in certain wavelength regions leading to a positive signal.
- Energy transfer (ET): a non-radiatively transmission of excite-state energy from one molecule to a close nearby molecule. This results in a positive signal.
- Non-radiative decay: multi phonons relaxation, resulting in heating of a sample.
- Product absorption: after the molecules have been excited a reaction may occur, which results in a transition or a long lived molecular state. Examples of these long lived molecular states are triplet states and charge-separated states. This results in a positive signal. Therefore intra- or intermolecular dynamics, electronic decay and vibrational relaxation can be observed.[2]

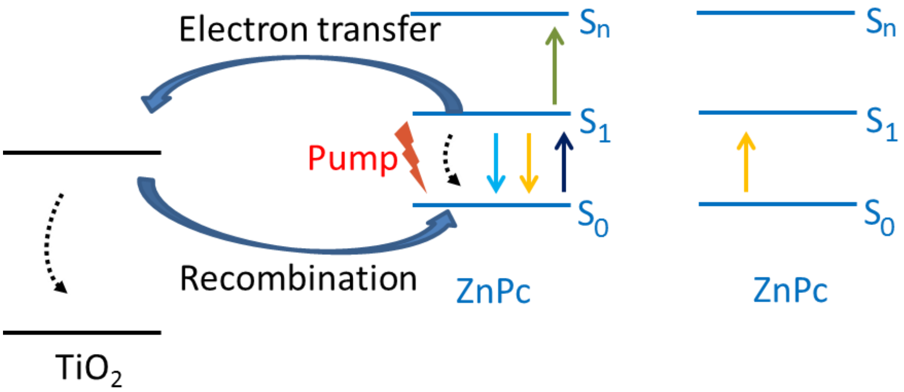

Figure 2.2 – Various processes contributing to a delta optical density spectrum: Ground state bleach: after excitation fewer molecules are in the ground state leading to less absorption of the ground state, thus a negative signal (Dark blue). Stimulated emission: certain wavelengths of the probe beam cause the molecule to relax to its ground state. More light falls onto the CCD camera, thus negative delta absorption signal (Blue). Spontaneous emission: even in absence of the probe light an excited state will eventual undergo a transition to a lower energy state. The lifetime depends on the properties of the molecule and

the mode structure of the surrounding medium. In quantum electrodynamics (QED) spontaneous emission is explained as stimulated emission through vacuum fluctuations. Light produced by spontaneous emission is called luminescence. Excited state absorption: after molecules are excited by the pump beam, higher excited transitions are possible by the probe. The intensity decreases, therefore a positive signal would be observed (Dark green). Energy transfer: a non-radiatively transmission of excite-state energy from one molecule to a close nearby molecule. This results in a positive signal (Orange). The black dotted arrow indicates decay paths of the electron.

2.1.3 Pulse duration

Time resolution in a transient experiment is limited by the duration of the pump and probe pulses. Usually the duration of a pulse is characterized by the full width at halve maximum (FWHM) as shown in Figure 3.1. Streak cameras are able to measure pulses of picoseconds. However to measure the duration of shorter pulses, correlation methods are required.

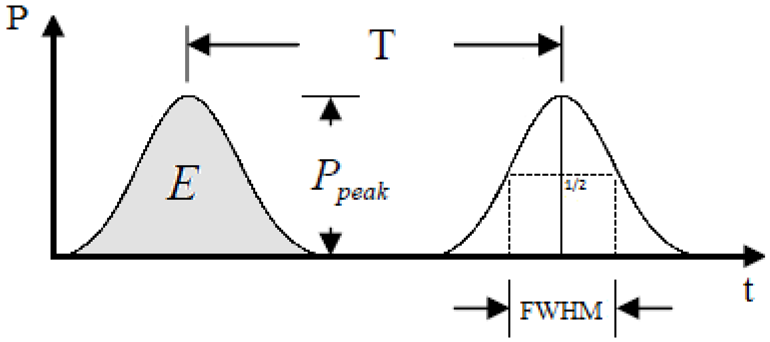

Figure 3.1 – Characterization of optical pulses. Shown are the FWHM, the period of the pulses T, pulse energy E and the peak power P_{peak}. The peak power of a pulse is inversely proportional with its time duration. Femtoseconds pulses provide very high peak power, making non-linear effects possible.

Autocorrelator

Pulses are characterized by the use of an intensity second harmonic autocorrelator. SHG is a non-linear optical process. In this process two photons interact with a non-linear crystal and are combined to one photon with a doubled frequency, as shown in Figure 3.2. The generated second harmonic photons must constructively interfere in the forward propagation which each other. This condition is called phase matching. This implies that $n(\omega) = n(2\omega)$. A birefringent crystal is usually used, it has two optical axes: an ordinary axis and an extra-ordinary axis, whose refractive index dependent beside on the wavelength also on the angle of the crystal. The thicker the non-linear crystal becomes, the higher the intensity of the second harmonic. However a ticker crystal has a smaller phase-matching bandwidth.

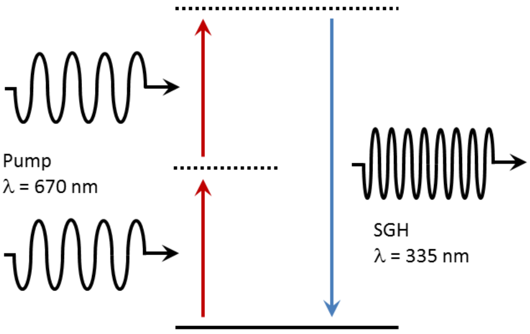

Figure 3.2 – Energy level diagram of second harmonic generation. Dotted lines represent virtual energy levels. Two simultaneous incoming photons excite an electron from the ground state to a virtual energy level, where it quickly drops down to the ground state. Thereby generating one photon with twice the frequency of the incoming photons.

In an intensity autocorrelation process the single light beam is split or reflected into two beams. One path is controlled delayed by computer software and both paths are spatially focussed into a birefringent material. When no temporal exists between both pulses, but the phase matching condition is hold, one might expect to see two second harmonic beams ($2\vec{K}_1$and $2\vec{K}_2$). When the two pulses also temporal overlap, a third second harmonic beam $\vec{K}_3 = \vec{K}_1 + \vec{K}_2$ can be observed. Because the intensity $\vec{K}_3$ depends on the temporal overlap between the two pulses, the pulse duration can be measured.

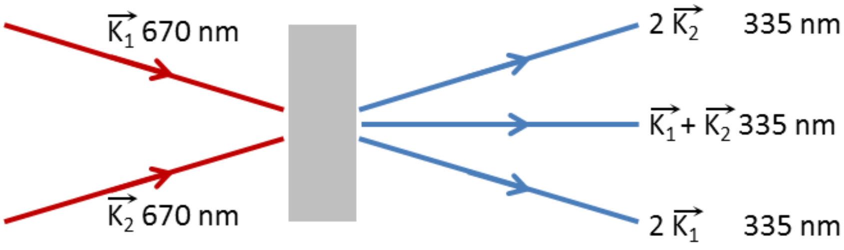

Figure 3.3 – Schematic representation of phase matching.

Autocorrelation is the correlation of a signal with itself, while cross correlation is the correlation of a signal with another (known) signal. One should not confuse correlation with convolution. The equation to calculate the convolution is $x(t) * y(t) = \int_{-\infty}^{\infty} x(\tau)y(t-\tau)d\tau$, while for correlation it is given as $x(t) \star y(t) = \int_{-\infty}^{\infty} x(\tau)y(t+\tau)d\tau$. A cross-correlation can be used to quantify the similarity of two signals, thus an autocorrelation can be used to examine a signal with itself. Signals can only be examined meaningfully using signals that are equally short or shorter, since the optical pulses are in the order of femtoseconds they can be examined using their own signal in an autocorrelation. Important is what the FWHM of an auto correlated pulse will be compared to the original pulse.

Since a convolution in the time domain is equal to a multiplication in the frequency domain; the Fourier transform of the auto correlated signal is a squared Fourier transform of the original pulse for a symmetrical pulse. Therefore the Fourier transform of a Gaussian pulse e^{-ax^2} is $\sim e^{-\frac{1}{a}\omega^2}$. The square of this is $e^{-\frac{2}{a}\omega^2} = e^{-\frac{1}{a}(\sqrt{2}\omega)^2}$. One can see that the FWHM of this Fourier transformed Gaussian is a factor $2^{0.5}$ smaller. When applying an inverse Fourier transform this gives the inverse effect thus an increase in FWHM of $2^{0.5}$.

3. Transient absorption setup

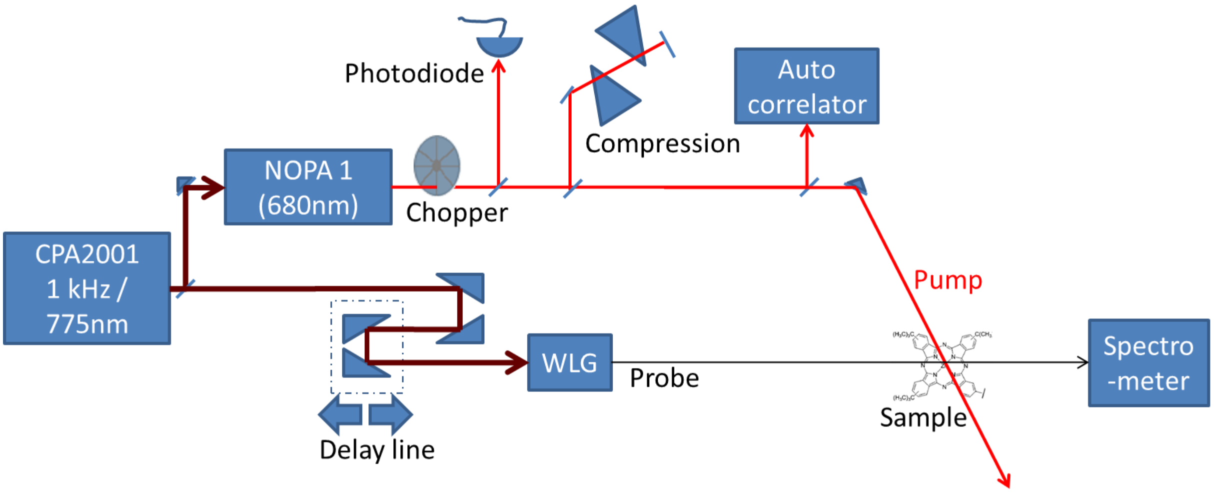

Figure 3.4 – Schematic representation of the transient absorption setup: The fundamental laser (CPA2001) produces near Fourier-transform-limited 150 fs pulses at a repetition rate of 1004 Hz. The centre wavelength is shifted to 670 nm, using a non-collinear optical parametric amplifier (NOPA). The pump beam is chopped at 502 Hz by a synchronised chopper. To compensate for the dispersion elements within the NOPA, pulse compression is applied to obtain near Fourier-transform-limited pulses. This compression is done using two prisms while monitoring the pulse duration by SHG-autocorrelation. The delay between pump and probe pulses is computer controlled by using a motorised delay line. The white light continuum (~460-700 nm) probe is generated by focussing the fundamental (775 nm) beam into a sapphire crystal. This probe measures the absorption of the sample in ground state and excited state for different time delays.

The hearth of a transient absorption setup, also called pump-probe (PP) setup, is a high power laser. In this laser ultra-short pulses of 150 fs are generated. The CPA2001 used for this project has a central wavelength of 774 nm and a repetition rate of 1004 Hz. The longest process one can observed is limited by this repetition rate, however long processes are not interesting for this project and the repetition rate of 1 kHz is sufficient. Commonly the pump and probe pulse, used in transient absorption measurements, are both generated from the same source, to minimise the effect of instability of the source. By carefully tuning a part of the fundamental beam in a non-collinear optical parametric amplifier (NOPA) this central wavelength is shifted to 670 nm, with a 30 nm spectral width and a near-Gaussian beam profile, so that the ZnPc can be excited. The pump beam gets modulated by a synchronised chopper and is compressed using prisms to regain near Fourier-transform-limited pulses of 22.7 ± 0.2 fs. The tuning of the prisms was done while monitoring the time duration, using a SHG-autocorrelator. Blindly using the prisms could even lead to broadening of the pump and probe pulses. After excitation of the sample the pump beam is blocked. Another part of the fundamental beam is guided through a computer-controlled delay line. The polarisation angle between probe and pump is set at 54.7 degrees, called the magic angle, to prevent anisotropy effects. This has been done with a $\lambda/2$ plate suitable for the wavelength of the fundamental. The fundamental is focused into a sapphire crystal to generate a white light continuum $^{(WLC)}$ of roughly 460 nm to 700 nm. This probe light is then focused onto the sample and guided afterwards to a spectrometer (diablo), homemade by AMOLF. The grating in this spectrometer has 1500 $\text{grooves}\cdot\text{mm}^{-1}$ and is blazed at 250 nm. The CCD inside the spectrometer has two array lines containing each 256 pixels. These pixels have a width of 50 μm, which results in a resolution of 1 $\text{nm}\cdot\text{pixel}^{-1}$. The CCD is sensitive for a range of roughly 200 nm to 1100 nm. Computer software controls the time delay between pulses and collects the data from the spectrometer and calculates the transient absorption signals. To average out some noise, 900 shots are averaged by the computer software. Figure 3.4 shows a simplified schematic.

3.1 Dynamic sample holder

The repetition rate of the CPA2001 is set at 1004 Hz. The synchronised chopper in the pump path is set at 502 Hz, therefore one pump pulse of the two pump pulses is blocked and one pump pulse per 2 mille seconds excites the sample (f_{rep}). An iris allows only the TEM00 mode of the pump beam, resulting in a Gaussian profile. By adjusting the last confocal mirror the special width of the pump beam at the focus point of the probe has been set. The FWHM sizes of the pump are set to 78.0 μm in vertical direction and 102 μm in horizontal direction (see appendix D), leading to a pump diameter (A_{pump}) of 6249 μm^2. The pump fluences Φ can be calculated by Equation 3.1.

$$\Phi = \frac{\mathrm{P}_{pump}}{E_{photon} * f_{rep} * A_{pump}}$$ **Equation 3.1**

The pump power (P_{pump}) was measured to amount to 10-11 $\mu\text{J}\cdot\text{s}^{-1}$ by a silica power detector. The central wavelength of the fundamental was shifted, using the NOPA, to 670 nm. One photon with a wavelength of 670 nm has photon energy (E_{photon}) of 296 zJ. Thus the samples have been excited by pump fluences of $1.08*10^{15}$ photons/ ($\text{pulse}\cdot\text{cm}^2$). And therefore the photons sees an area of $9.23*10^{-16}$ cm^2. Literature value of the cross section of ZnPc is $1.50*10^{-16}$ cm^2, [8] given a ratio of only 6, however by experimental is verified the power to be still in the linear regime.

To ensure the sample does not locally bleach, a dynamic sample holder has been built. Without dynamic sample holder, bleaching is observed within minutes. To be able to build a cheap controllable translation stage, 5 CD-players were dismantled. The translations for these CDread heads were controlled by simply putting a block signal on the DC motor. The stability of such a system was checked by shining a HeNe laser through a mounted glass slide at 45 degrees incidence. By watching the displacement of the reflection, conclusions could be made on the stability. A few mm deviations were observed, which rendered this idea useless.

To make a more robust controlled translation stage, a manual translation stage was used. A screw motor was placed for one x axis and a platform for the sample was fabricated in the workshop. The maximum velocity at which the translation stage can be moved is 0.3 $\text{mm}\cdot\text{s}^{-1}$. Therefore 250 pulses excite the sample per second. The z-movement can be manually controlled by two axes, making a 2.4 cm movement possible. The focussing in y-direction can be adjusted by a manual translation stage able to move 1.6 cm. The movement in x-direction can be automatically controlled 1.2 cm. This is done using two end switches, a motor and a flip-flop circuit. The holder moves from one end to the other. Manually one can move 1.6 cm in x-direction. For schematics of electronics see appendix A.

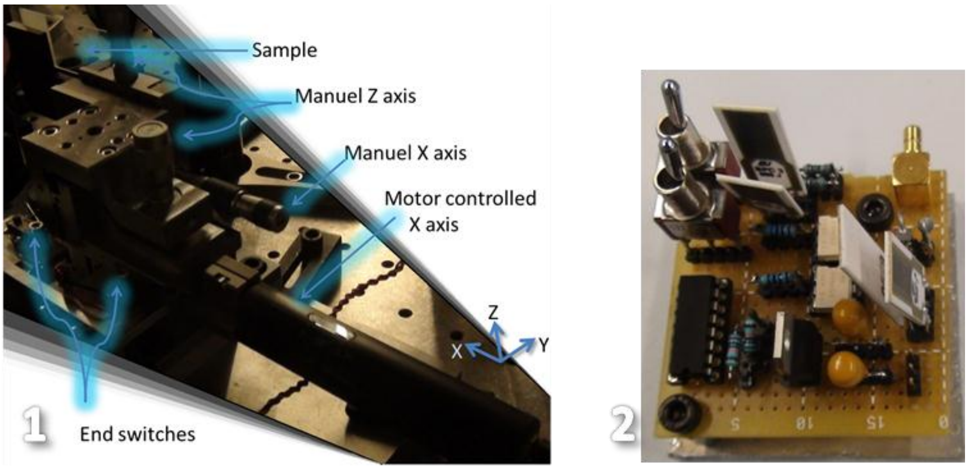

Figure 3.5 – (1) Automated translation stage using a CMA12CC linear actuator. (2) Electronics for automatic translation stage.

3.2 Fluctuation in pump power

The processes in a system one wants to measure depends upon the amount of photon it is absorbing. Thus the transient absorption signal depends on the amount of pump power. The power needs to be set at a certain value range in order to do a right experiment. In our setup a small fraction of the pump beam is reflected by the same neutral density filter $^{\text{(NDF)}}$ used to set the power. A photodiode measures the intensity of the reflected part of the pump beam. Using computer software, boundaries can be set for which data are recorded.

3.3 Autocorrelator

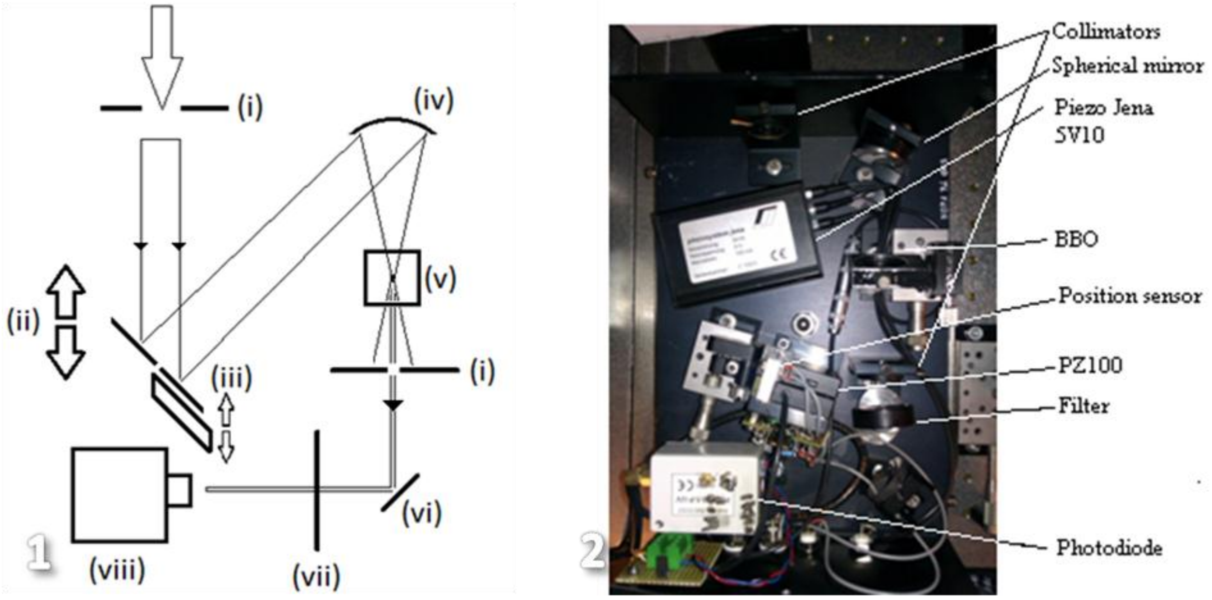

Figure 3.6 – Schematic (1) and photograph (2) of SGH-autocorrelator: (i) irises, (ii) translation stage, (iii) piezoelectric element, (iv) focal mirror, (v) BBO crystal, (vi) mirror, (vii) colour filter-SP440, (viii) photodiode.

Figure 3.6 shows the arrangement of the SGH-autocorrelator setup. Two irises to align the laser beam are placed strategic in the setup (i), also blocking direct background light. Refractive optical elements cause pulses to broaden. Thus instead of a beam splitter, a mirror consisting of two pieces was used. One piece (ii) is fixed on an adjustable translation table and the other part (iii) is put on a piezoelectric element (PZ100) for an adjustable time delay. A spherical mirror (iv) is used for focusing the laser beam into the Barium borate (BBO) crystal with thickness 20 μm (v), which generates a second harmonic if spatial and temporal overlap of the two beams is achieved. A coated mirror (vi) reflects the beam through a colour filter (vii), which passes only the second harmonic, into the (Becker & Hickl GmbH) photodiode PDI 400 1 P-UV (viii). This detector has a slow response to the light pulses allowing for measurements of the average light intensity. The photodiodes peak response is around 3.5 μs after impact of the light pulse. In LabVIEW the triggering is used to measure this peak response. The piezoelectric element (Piezosystem Jena GmbH) PZ100 can provide a delay of 600 fs to ensure that the entire pulse is obtained. The fact that a position sensor is used in the autocorrelation allows the user to oscillate repeatedly the PZ100 and do a series of measurements on the same pulsed signal. These measurements can be averaged out for a better signal to noise ratio (S/N).

FROG

By using a spectrometer instead of a photodiode also spectral information is gained. Therefore frequency resolved optical gating (FROG) is a spectrally resolved autocorrelation. To measure the probe pulse duration of a transient absorption commonly a cross-FROG (XFROG) is used. In such a setup, the duration of the pump pulses are known, while the duration of probe pulses are unknown. The probe and pump pulses are spatially overlap on a dye which a large absorption cross-section for two photon absorption. To examine a WLC probe pulse with a pump pulse of 650 – 700 nm an ultra violet dye is needed, for example Hoechst 33258.

3.4 Prisms compression

An optical pulse is composed out of many frequencies, which have a certain phase relationship, such that at the periodic time interval all phases are equal. On such an interval all waves constructively interfere resulting in a high energetic pulse. Chirp is the phenomenon of time dependence on when a wavelength of a pulse arrives, resulting in longer pulses. Linear pulse dispersion (linear chirp) introduced to Fourier transformed limited pulses by optical elements like filters and lenses, can be compensated by a pair of prisms. Some other methods of linear pulse compression on these optical ultra-short pulses (pulses with time duration of picoseconds or less) are: a grating compressor, an optical fiber and a chirped mirror. In order to recover near bandwidth-limited pulses, the pulses are sent through an optical element with a chromatic dispersion suitable for flattening the spectral phase of the incoming pulses, hence removing the chirp on the pulses.[29]

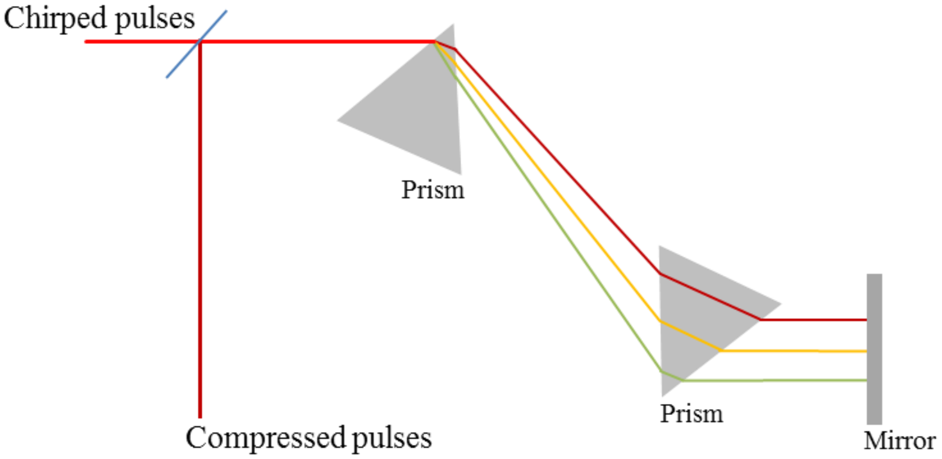

Figure 3.7 – Prisms compression.

4. Sample preparation

The sample preparation consists of two main parts:

1. The preparation of a TiO_2 film or an Al_2O_3 film. These films need to be as homogenous as possible. Thus the films need to be smooth, without cracks and transparent for visible light.
2. The preparation of the solution, consisting of the dye, ethanol and chenodeoxycholic acid (cheno). The cheno was purchased from Sigma Aldrich. A complete sample consists of a glass slide coated with a nano crystalline and nano porous TiO_2 film. On this film the dye is anchored, as shown in Figure 4.1.

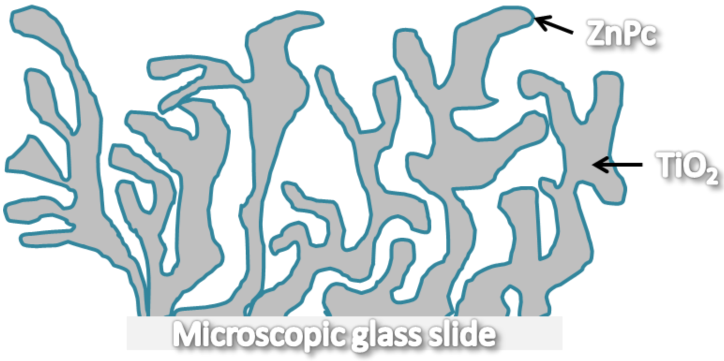

Figure 4.1 – Schematic representation of the samples consisting of a microscopic 1mm glass slide on which a nano porous crystalline thin TiO_2 film is deposited. One of the novel ZnPcs is anchored on this film.

4.1 Part 1: TiO_2 film and Al_2O_3 film

In order to produce smooth, crack free TiO_2 films proper clean materials need to be used. Also the environment needs to be cleaned. Gloves need to be worn at all times during the sample preparation, this to prevent contamination of the oven and the slides. The TiO_2 nanoparticles are relative safe to work with, for they are deposited on a glass slide by a paste. Still because of their sizes, wearing gloves is also necessary to prevent them to cause serious health issues.

In a DSSC the titanium dioxide film would consist of many different particles sizes to induce scattering leading to longer optical paths in the DSSC. However transient absorption measurements are impossible for high scattering materials. Therefore, we use TiO_2 consisting of only small particles, leading to a higher transparency. Paste with small particles (diameter 8-10 nm) was ordered from Solaronix (Ti-Nanoxide HT). The 1 mm glass slides and pipettes have been ordered from VWR.

The first step to create a TiO_2 film on top of a glass slide is to tape the clean glass slide on a clean table, as is indicated in Figure 4.2.

Figure 4.2 – Taping five clean glass slides onto a clean surface.

Some force was applied on the edges of the tape with a finger to make the height well defined. The bottle, containing the paste, had to be sonicated for roughly 30 minutes. The sonication was done by a commercial ultra-sonic cleaner, Brandson 1510. After this sonication the paste was stirred by using a glass pipette and stricken at the surface of another glass pipette while rotating it, as shown in Figure 4.3 (1 and 2).

Figure 4.3 – Applying TiO_2 nanoparticles onto a pipette.

Most of the liquid was deposited at the edge of the glass slide, by rotating the pipette, as done in Figure 4.4(1). Afterwards, the liquid had to be distributed over the glass slide. This was done by moving the pipette up and down, as is shown in Figure 4.4(2), while applying force downwards. This step had to be performed quickly in order to create a homogenous TiO_2 film. The tape can be removed now, as shown in Figure 4.4(3, 4). If for some reason this process is delay, the TiO_2 film will show cracks near the edges. The TiO_2 film will become transparent within five minutes.

Figure 4.4 – Applying the TiO_2 nanoparticles to the glass slide.

After one day dust free storage, the samples were sintered in a Nabertherm B180 oven under standard conditions at 450° C for 30 minutes. By doing this the organic binder is removed, leaving a nano porous TiO_2 film and creating inter-particle connection. After the samples had gradually cooled down to 80° C they had to be checked on cracks. This had to be done quickly to prevent the TiO_2 film from absorbing moisture in the air. The most homogenous TiO_2 film was bathed still roughly at 80º C in a solution consisting of ethanol, co-solvent cheno and TT1, TT6, TT7 or TT15. The thickness of the TiO_2 film is expected to be roughly 4 μm, for the same procedure described in reference [5] is followed to make the TiO_2 films.

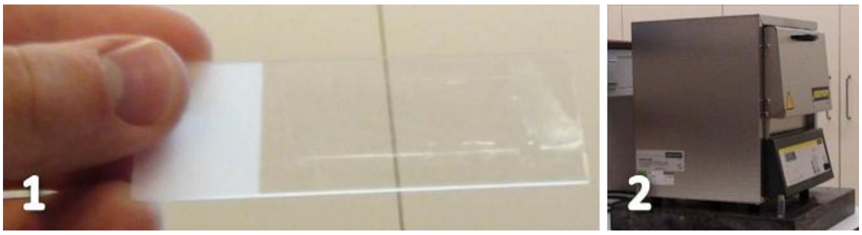

Figure 4.5 – (1) TiO_2 film a few minutes after being made and (2) furnace used for annealing.

4.2 Part 2: Preparation of solution and working towards a sample

The first step to make the solution, consisting of 20 mM of cheno with 0.07-0.08 mM of dye, is done by putting 78.5 mg cheno and 0.6 mg dye into a clean and empty 30 mL glass bottle. The quantities are measured by a pioneer^{TM} analytical and a precision balance of OHAUS. This balance is able to measure weights with an uncertainty of ± 0.1 mg.

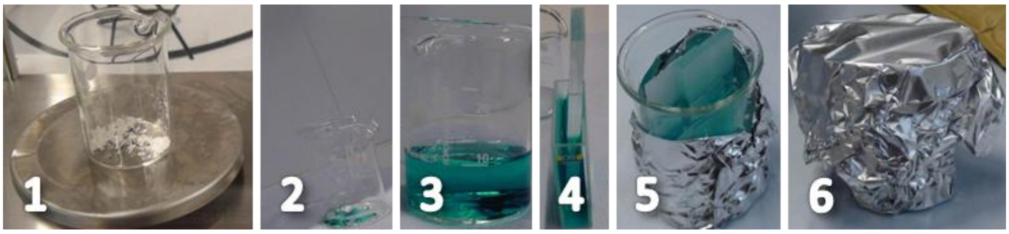

Figure 4.6 – Preparation of solution.

After weighing of the powders, the beaker is filled with 10 mL ethanol (Ethanol absolute AnalaR NORMAPUR® ACS ordered from VWR). This ethanol contains very few heavy metals, for they can influence the pump-probe measurements. After the solution has been sonicated, a small portion is kept in a small bottle. This portion is used for steady state absorption to ensure the weighting has been done properly. To increase to solution height five clean glass slides are inserted in the beaker.

Figure 4.7 – Small portion of solution used for steady-state absorption measurements.

After the steady-state absorption measurements, the small portion is put into a small bottle for storage. When the solution absorption spectrum shows no abnormalities, the best TiO_2 film (one with a nearly perfect homogenous film) is put in the solution. There it remains for 240-270 minutes, surrounded by aluminium foil to block light.

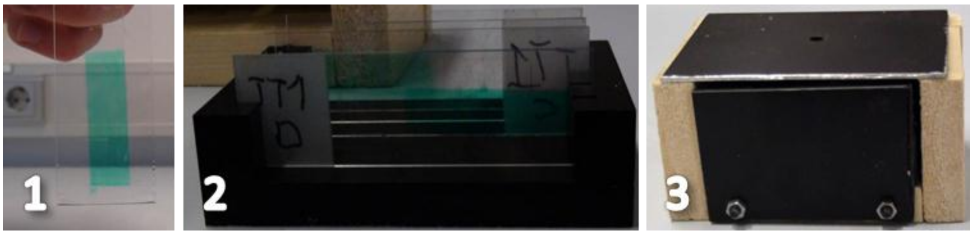

Figure 4.8 – Storage of the samples.

After those four hours the sample is cleaned five times with the pure ethanol, using a pipette. This washes off all zinc-phthalocyanine that has not been anchored on the titanium dioxide film. A monolayer of the dye is now anchored onto the nano porous TiO_2 film. The sample is ready to be used and has to be labeled. During transient absorption measurements, without a moving automated translation state, bleaching was observed of the molecules. The degradation of molecules is mainly due to the formation of singlet oxygen. [24] For this reason the samples were stored in a nitrogen purged box, shown in Figure 4.8(3).

Al_2O_3 film preparations

To prepare the Al_2O_3 paste, the same preparation steps have been taken as described in Ref [5]. Al2O3, < 50 nm particle size and 50 wt. % in isopropanol were purchased from Sigma Aldrich together with 5 gram hydroxypropyl cellulose (powder). 15 mL of the colloidal dispersion was heated to 65º C. Using the precision balance of OHAUS 0.35 g of hydroxypropyl cellulose is weighted and is added to the heated colloidal dispersion. Using a glass stirring rod the mixture is stirred properly. A magnetic stirring rod is used to stir the mixture continuously for five days. To compensate for evaporation, milli Q water is added at regular times. After the five days the paste is ready to use in the same way the TiO_2 paste is used to make a film.

5. Results and discussion

- Paragraph 5.1 shows steady-state measurements recorded with the shimadzu UV 1800 spectrometer. A resolution of 2 nm was used for the experiments. The spectrometer is able to record absorption spectra for 190 nm to 1100 nm. For this the device has two lamps made out of different materials: wolfram and deuterium.
- Paragraph 5.2 shows the measurements done with the transient absorption setup.

5.1 Steady-state measurements

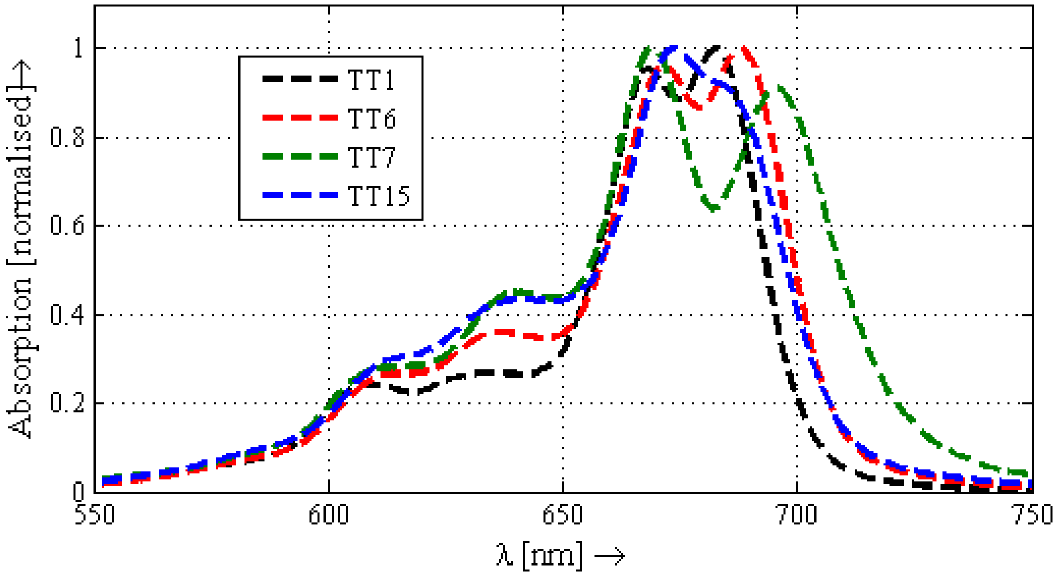

Figure 5.1 – Absorption spectra of TT1, TT6, TT7 and TT15 in ethanol (0.7 mM) and co-solvent cheno (20 mM) solution.

Absorption spectra have been acquired for the four novel ZnPcs in solution. The solvent is ethanol, containing 20 mM cheno. In Figure 5.1 vibronic bands are observed around 600-650 nm, the split Q-band is observed around 650-750 and contribution of aggregation, typically the dimer, is appearing around 620-650. The co-solvent cheno is known for its ability to suppress the formation of aggregation. To compare fairly the novel ZnPcs the same concentration of cheno has been used.

Luminescence was measured at room temperature, using an excitation wavelength of 606 nm for all 0.7 mM novel ZnPcs in an air-equilibrated ethanol, with 20 mM co-solvent cheno. The data is shown in Figure 5.2.

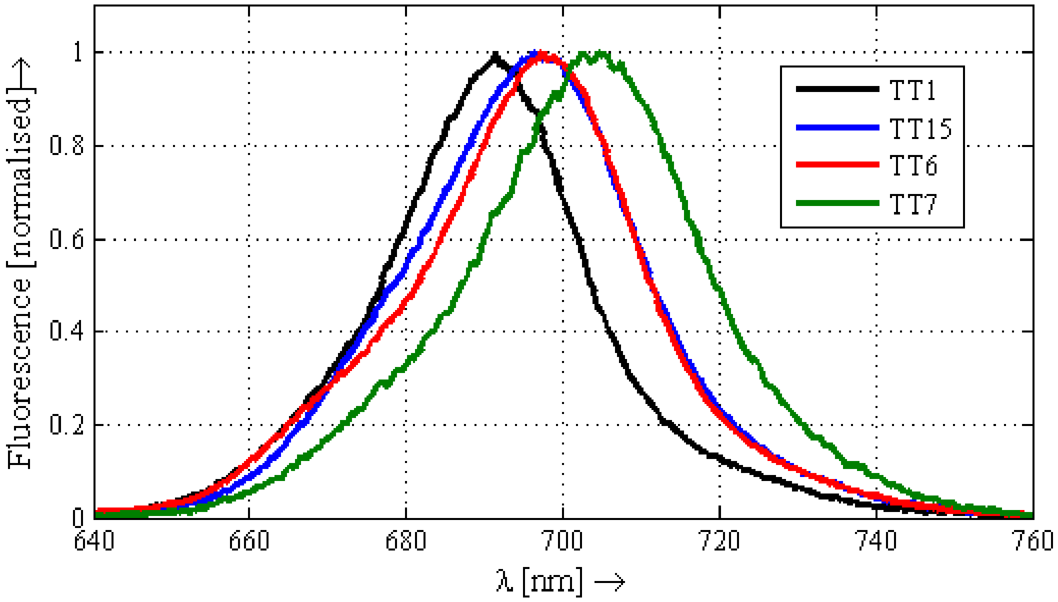

Figure 5.2 – Fluorescence spectra of TT1, TT6, TT7 and TT15. λ_{ex} = 606 nm

The profiles of the fluorescence spectra are similar for TT1, TT6, TT7 and TT15 with respectively luminescence maxima at 691 nm, 697 nm, 698 nm and 704 nm. Earlier reported luminescence maximum for TT7 was given as 700nm, [1] which is close to the measured value.
The absorption spectra of TT1, TT6, TT7 and TT15 anchored onto TiO_2 are shown in Figure 5.4. TT1 and TT7 anchored onto Al_2O_3 are shown in Figure 5.5.

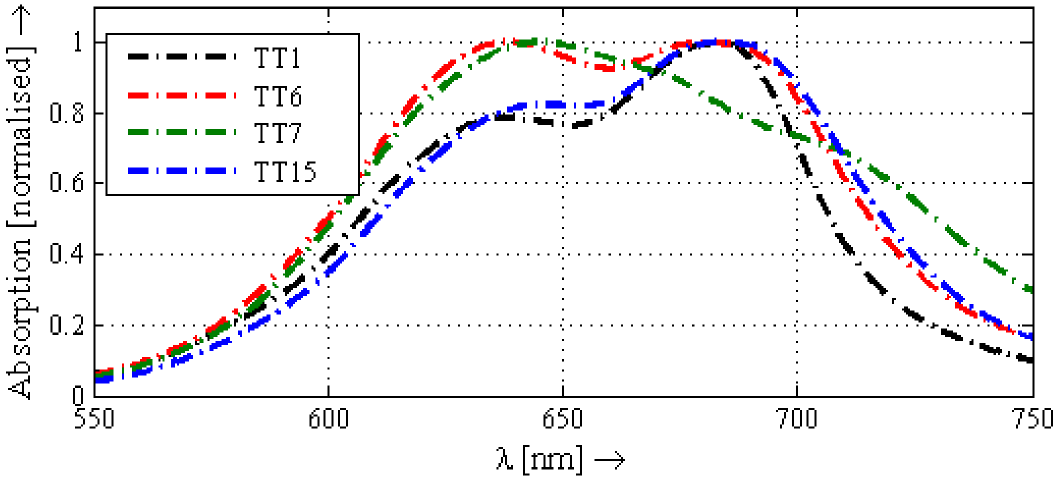

Figure 5.3 –Absorption spectra of TT1, TT6, TT7 and TT15 adsorbed onto a nano crystalline transparent TiO_2 film.

For all spectra of TT1, TT6, TT7 and TT15 substantial broadening is observed. This indicates that a strong electronic coupling exists between the novel ZnPcs and the TiO_2 film. The over-all profile of TT7 has changed. Reason for this might be the presence of the CN group. The maxima absorption peaks are located at:

- TT1-TiO_2 at 637 and 684 nm, TT1-Al_2O_3 at .631 and 678 nm
- TT6-TiO_2 at 638 and 681 nm.
- TT7-TiO_2 at 645, TT7-Al_2O_3 at 644 nm.
- TT15-TiO_2 at 645 and 684 nm.

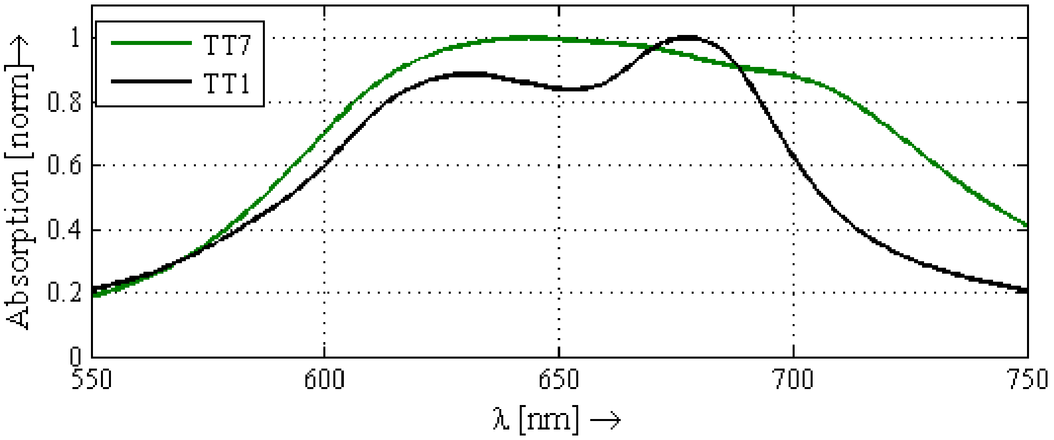

Figure 5.4 –Vis absorption spectra of TT1, TT6, TT7 and TT15 adsorbed onto a nano crystalline transparent Al_2O_3 film.

More scattering can be expected due to the imperfect film of Al_2O_3 and thus a higher background signal, as seen in Figure 5.4. The spectrum for the sample of TT1-Al_2O_3 shows a shift of 6 nm compared to the spectrum of TT1-TiO_2.

5.2 Time-resolved measurements

In a transient absorption measurement time shots are taken of the excited state of the system of interest. The measurement time per dataset is 10 minutes. The data can be shown as a 2d plot: the x-axis presents the probe wavelength and the y-axis presents the time delay between pump and probe pulse. In Figure 5.5 the data is shown for TT1-TiO_2 and TT1-Al_2O_3. The 2d data plots of TT6-TiO_2, TT7-TiO_2, TT7-Al_2O_3 and TT15-TiO_2 can be found in appendix E. The z-axis presents the amplitude of the ΔOD signals and for a 2d plot is given as a colour. To increase the signal to noise ratio, multiple data sets are taken. First the time zero is set correct for all of these data sets and the background signal is subtracted in order to average them. To do a global analysis the chirp of the system also needs to be corrected, however this has not been done yet.

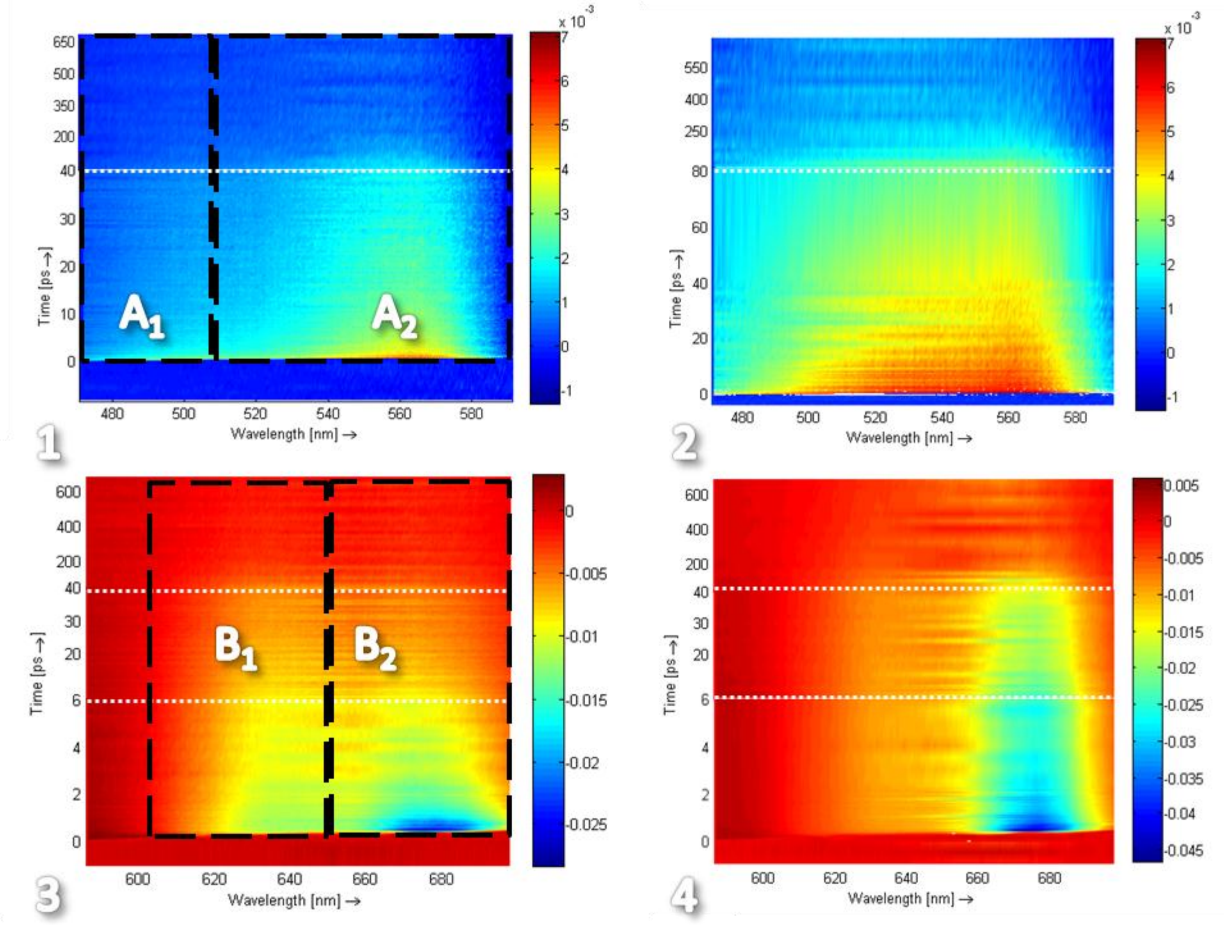

Figure 5.5 – Transient absorption measurements of TT1 anchored on $^{(1,\ 3)}$ TiO_2 and anchored on $^{(2,\ 4)}$ Al_2O_3. Processes contributing to the transient absorption measurement are indicated as followed: (A_1) ESA (A_2) Overlap of ESA and charge separated state (formation of ZnPc radical cation) (B_1) overlap SE and GSB originating from the dimer and (B_2) from the monomer. TT1-Al_2O_3 exhibits much slower dynamics. By vertical crossing of a white dotted line, a different time scale is applied to enhance the readability of the 2d data plot.

Transient absorption measurements of TT1-TiO_2 and TT1-Al_2O_3 are shown in Figure 5.5(1, 3) and Figure 5.5(2, 4). The measurements on TT1-Al_2O_3 were done to see clearly the dynamics of electron injection (EI) and recombination. For this metal oxide has a higher conduction band, therefore EI is prevented. TT1 anchored onto TiO_2 exhibits much faster dynamics as compared to TT1-Al_2O_3.

The following contributions have been indicated in the 2d plots of Figure 5.5:

- (A_1) ESA of ZnPc
- (A_2) Overlapping of ESA and charge separated state: formation of $ZnPc^+$. The radical cation in solution is known to absorb at centre wavelengths of 825, 720, 500, 440 and 321 nm.[23] However the positive band around 560 nm can be assigned to the $ZnPc^+$.[25]
- Overlapping of stimulated emission (SE) and ground state bleach (GSB) signals from the dimers (B_1) and from the monomers (B_2). As previously shown in the steady-state measurements, TT1 in solution exhibits a maximum fluorescence at 690 nm and TT1 anchored onto TiO_2 exhibits absorption maxima at 637 and 684 nm. TT1-TiO_2 and TT1-Al_2O_3 have both been excited at 670 nm (30 nm FWHM) and a high degree of GSB can be expected at these probe wavelengths. The minima peaks of ΔOD were located at 642 and 678 nm. Signals from SE processes are expected to be Stokes shifted as compared to GSB. If the GSB signals and the SE signals are overlapping, then a Stokes shifted of 5-6 nm is observed.

By plotting the ΔOD versus wavelength at different time delays snapshots of the spectrum are taken to see the evolution of the spectrum. Figure 5.6 is shown as an example.

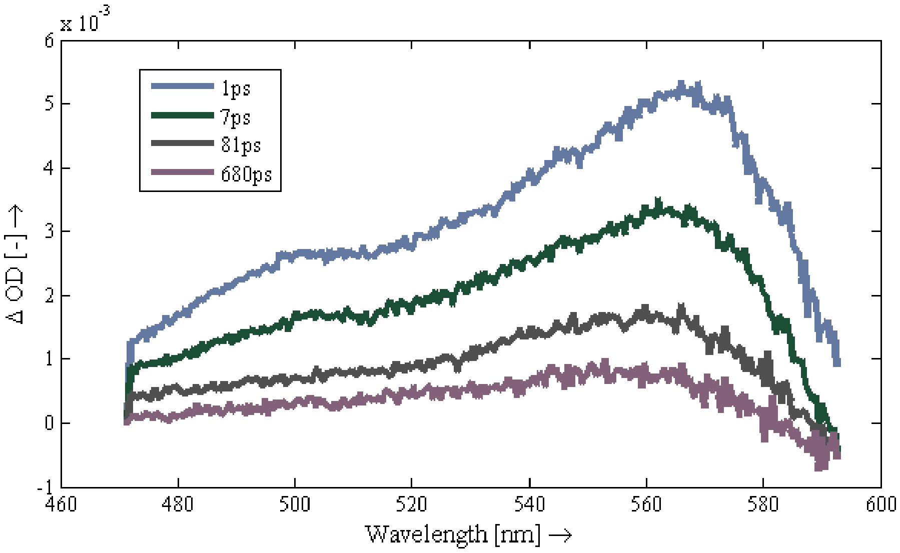

Figure 5.6 – Evolution of the spectrum (TT1-TiO_2) ranging from 1 ps to 680 ps.

Another analysis tool is to plot the ΔOD versus delay time for certain wavelengths. The decay of ESA is a measure on which timescale electrons are injected into the TiO_2 conduction band, Wavelength 500 nm shows primarily ESA signal and is therefore a good choice for the EI rate analysis. To observe the recombination of electrons from the TiO_2 conduction band to the ground state of the cation, one can look at the dynamics of the GSB recovery. The wavelength chosen for analysis is 650 nm, because for wavelengths smaller than 650 nm a higher signal of the dimers is observed and for higher wavelengths the signal of SE is increased.

To fit the data a bi-exponential decay curve is used. As explained in the introduction a two component decay is expected for EI due to ‘hot’ and the relaxed excited state. To take into account dye molecules which do not inject an offset is added.

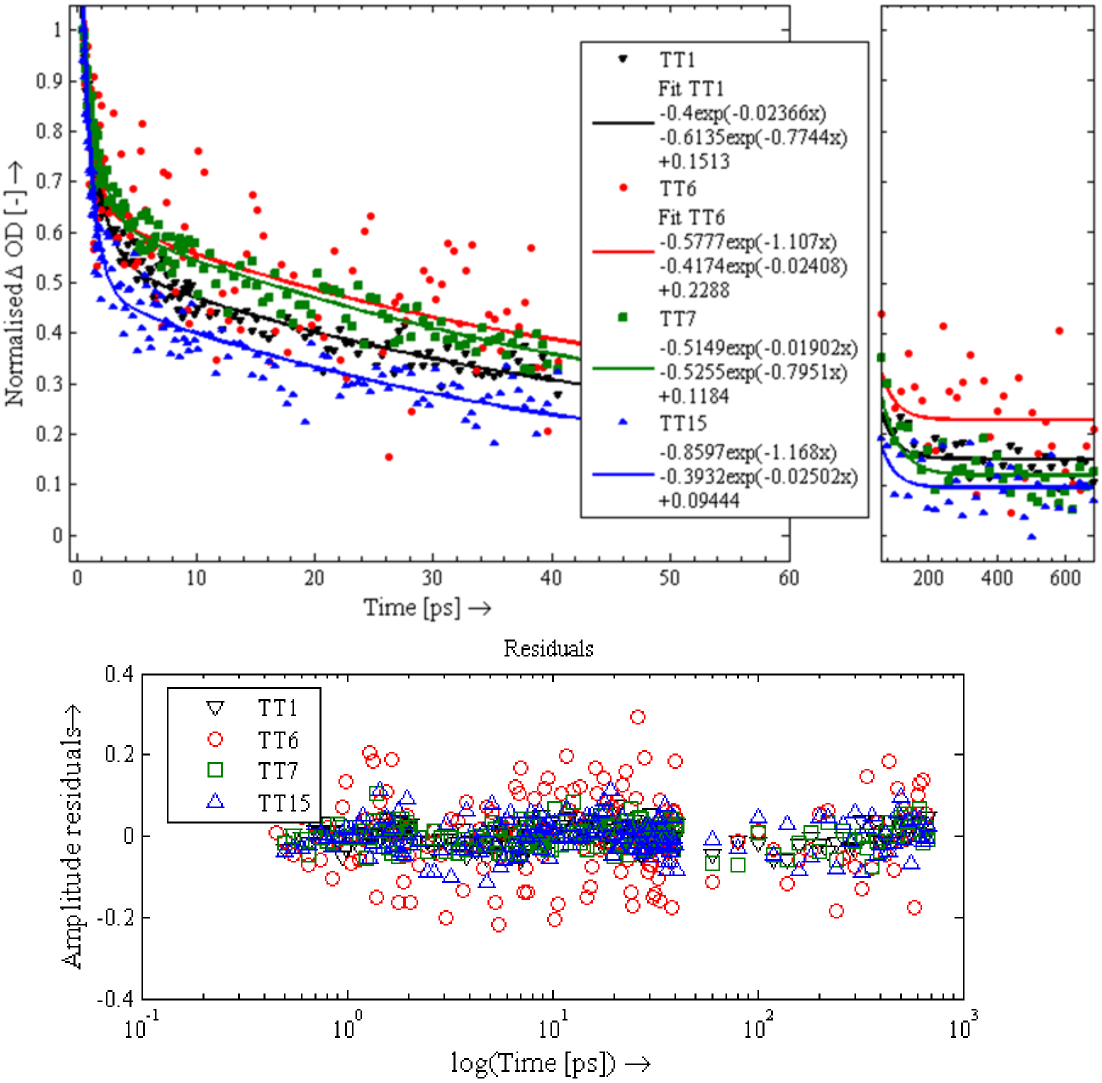

Figure 5.7 – Decay of ESA signal at λ = 500 nm.

From these bi-exponential fits the lifetime components of the novel ZnPc are extracted. The data are fitted as can be seen from the residuals plot in Figure 5.7, though TT6 has twice the amount of amplitude of residuals compare to the other derivatives of ZnPc.

- TT1: τ_1= 1.29 ± 0.16 ps , τ_2= 42.27 ± 4.38 ps
- TT6: τ_1= 0.90 ± 0.70 ps , τ_2= 41.53 ± 16.42 ps
- TT7: τ_1= 1.26 ± 0.23 ps , τ_2= 52.58 ± 5.56 ps
- TT15: τ_1= 0.86 ± 0.15 ps, τ_2= 39.97 ± 6.51 ps

The ‘hot’ EI rates of TT1 and TT7 are roughly equal for both TT6 and TT15. The EI rate from the relaxed excited state seems to be ~1.2 times slower for TT7. The extra COOH group of TT15 compared to the one COOH group of TT1, seems to force the dye into a different orientation towards to semiconductor resulting in a higher electronic overlap between donor and acceptor. This would explain the higher EI rate. The impact of the CN group of TT7 can be seen by comparing TT7 with TT6. The presence of the CN group was expected to increase the EI rate; however these data show the opposite.

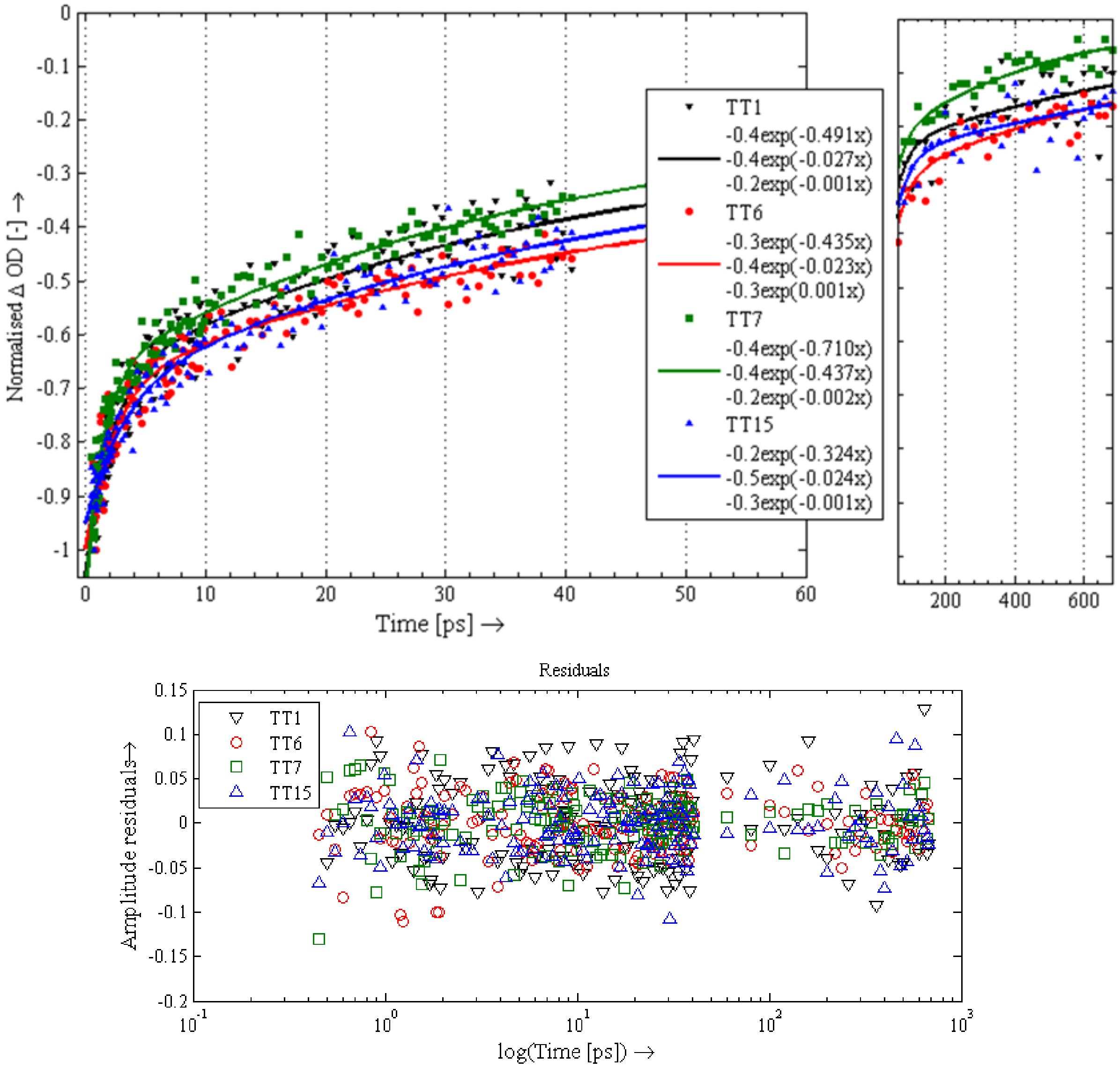

Figure 5.8 – Recovery of GSB at λ = 650 nm

From the tri-exponential fit the recovery lifetime of the GSB is extracted. A tri-exponential fit has been chosen, because no good fitting parameters could be found for a bi-exponential fit.

- TT1: τ_1= 2.04 ± 0.89 ps, τ_2= 37.17 ± 11.99 ps τ_3= ~1 ns
- TT6: τ_1= 2.30 ± 0.85 ps, τ_2= 44.44 ± 12.59 ps τ_3= ~1 ns
- TT7: τ_1= 1.41 ± 0.33 ps, τ_2= 32.82 ± 7.09 ps τ_3= 452.59 ± 156.63 ps
- TT15: τ_1=3.09 ± 1.61 ps, τ_2= 41.70 ± 11.25 ps τ_3= ~1 ns

TT7 anchored onto TiO_2 shows the quickest recovery of the ground state bleach. This can be explained by the CN group. The TT7 dye based DSSC has the lowest efficiency of the four ZnPc derivatives. It appears that the efficiency of the DSSC drop significantly if recombination rates are close to the EI rates.

The fast component is due to electrons which had been injected into the TiO_2 film, but remain close to the dye molecule. The third component is a rough estimate, because longer time delays are required to accurate quantify this component. TT15 shows the slowest recombination rate, indicating a deeper electron injection as compare to the other ZnPcs.

6. Conclusions and recommendations

6.1 Conclusions

Influences of anchoring groups

	Bridge	Electron injection rates $^{(\lambda = 500\ \mathrm{nm})}$	Recombination rates $^{(\lambda = 650\ \mathrm{nm})}$
TT1-TiO_2 η = 3.56 %		τ_1= 1.29 ps, τ_2= 42.27 ps	τ_1= 2.04 ps, τ_2 = 37.17, τ_3= ~1 ns
TT6-TiO_2 η = 3.28 %	$HC=CH$	τ_1= 0.90 ps, τ_2= 41.53 ps	τ_1= 2.30 ps, τ_2 = 44.44 ps, τ_3= ~1 ns
TT7-TiO_2 η = 2.55 %	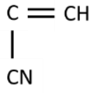 $\begin{array}{l}C=CH\\ \vert\\ CN\end{array}$	τ_1= 1.26 ps, τ_2= 52.58 ps	τ_1= 1.41 ps, τ_2 = 32.82 ps, τ_3= 452.59 ps
TT15-TiO_2 η = 3.96 %	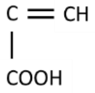 $\begin{array}{l}C=CH\\ \vert\\ COOH\end{array}$	τ_1= 0.86 ps, τ_2= 39.97 ps	τ_1= 3.09 ps, τ_1 = 41.70 ps, τ_1= ~1 ns

Table 6.1 – Electron transfer rates of the four novel ZnPcs

By comparing the electron transfer rates of TT1 and TT6, one would expect a higher efficiency for TT6. This would mean that through to the bridge, and thus a longer distance between donor and acceptor, the EI rate would increase and lower recombination rate. However the measured efficiency of TT6 is in fact lower than TT1, because of this inconvenience nothing can be said of the impact of a longer linker on the electron transfer rates.

The CN group of TT7 was expected to promote the electron pulling character of the linker resulting in higher electron transfer in both directions, however only higher recombination rates were observed. The efficiency of a DSSC is decreased considerably when the recombination rate is close to that of the EI rate as can be seen by comparison of TT1 and TT7.

The extra COOH group of TT15 compared to the one COOH group of TT1 seems to force the dye into a different orientation towards to semiconductor resulting in a higher electronic overlap between donor and acceptor. This would explain the higher EI rate, which in combination with the lower recombination rate results in higher efficiency in comparison with TT1.

Technical improvements

The transient absorption setup has been improved by:

- The homebuilt automated sample holder. Through this automated translation table sample degradation can be avoided for samples placed on a microscopic glass slide.
- Fine alignment of the optical paths and alignment into an autocorrelator.

- The amount of signal fluctuation in our transient absorption signal depends on the quality of the TiO_2 film. Smooth TiO_2 films have been produced and also transparent films of Al_2O_3 have been made, though latter films show lots of cracks.
- A nitrogen purge storage, samples could be stored for more than a week. However samples older than 2 days were avoided to use.

6.2 Recommendations

Influences of anchoring groups

Global analysis can be used to extract the pathways and efficiencies of the competing relaxation processes from the excited state, together with lifetimes and excited-state absorption spectra. A very good software program to do just this is ‘Glotaran’. Due to the finite time reserved for this work, I only worked two days with this program. Some primarily analysis were achieved, but these results are not used.

Technical improvements

To improve even further the automated sample holder the movement could be made random, so that the periodicity in the transient signal can be avoided. Also nitrogen can be purged onto the sample to avoid generation of singlet oxygen responsible for damaging the sample.

A vast improvement to the transient absorption setup would be to be able to automatically block the pump after the measurement. This can be achieved relative easily by placing a controlled shutter in the pump path and small tweaks have to be made to the lab view program used to measure a transient absorption run.

It would be interesting to have a quantitatively measurement on the quality of the films of TiO_2 and Al_2O_3 films, for example by measuring the surface with a profile meter.

The white light beam travels through two lenses: one to collimate the beam after WLG and one to focus the probe beam onto the sample, However these two lenses are causing significant amount of chirp. The white light is spectrally broad (~460-700 nm) and observed chirp was $6.23\ fs\cdot nm^{-1}$. The two lenses could be replaced by parabolic mirrors, hence reducing the chirp of the system.

7. Abbreviations

AM	Air mass
CCD	Charged coupled device
Cheno	Chenodeoxycholic acid
DSSC	Dye Sensitized Solar Cell
ESA	Excited state absorption
FROG	Frequency-resolved optical gating
FTO	Fluorine-doped tin oxide
FWHM	Full width at half maximum
GSB	Ground state bleach
ITO	Indium tin oxide
LUMO	Lowest unoccupied molecular orbit
NDF	Neutral density filter
NOPA	Non-collinear optical parametric amplifier
OD	Optical density
SHG	Second harmonic generation
TL	Transform limited
WLC	White light continuum
ZnPc	Zinc-phthalocyanine

References

[1] Miguel García-Iglesias, Juan-José Cid, Jun-Ho Yum, Amparo Forneli, Purificación Vázquez, Mohammad K. Nazeeruddin, Emilio Palomares, Michael Grätzel, Tomás Torres. *Increasing the efficiency of zinc-phthalocyanine based solar cells through modification of the anchoring ligand*, Energy & Environmental Science **2001** 4(1), 189-194

[2] Rudi Berera, Rienk van Grondelle, John T. M. Kennis. *Ultrafast transient absorption spectroscopy: principles and application to photosynthesis systems*, Photosynth Res. **2009** 101(2-3), 105-118

[3] Janne Savolainen, Dennis van der Linden, Niels Dijkhuizen, Jennifer L. Herek, *Characterizing the functional dynamics of zinc phthalocyanine from femtoseconds to nanoseconds*, Journal of Photochemistry and Photobiology A: Chemistry **2008** 196, 99-105

[4] Elena Galoppini, *Linkers for anchoring sensitizers to semiconductor nanoparticles*, Coordination Chemistry Reviews **2004** 248(13-14), 1283-1297

[5] Juan-José Cid, Miguel García-Iglesias, Jun-Ho Yum, Amparo Forneli, Josep Albero, Eugenia Martínez-Ferrero, Purificacíon Vázquez, Michael Grätzel, Mohammad K. Nazeeruddin, Emilio Palomares, Tomás Torres. *Structure-Function Relationships in unsymmetrical Zinc Phthalocyanines for Dye-Sensitized Solar Cells*, Chemistry **2009** 15(20), 5130-5137

[6] Ashis K. Sarker, Man Gu Kang, Jong-Dal Hong. *A near-infrared dye for dye-sensitized solar cell: Catecholate-functionalized zinc phthalocyanine*, Dyes and Pigments **2012** 92(3), 1160-1165

[7] Mohammad K Nazeeruddin, Filippo De Angelis, Simona Fantacci, Annabella Selloni, Guido Viscardi, Paul Liska, Seigo Ito, Bessho Takeru, Michael Grätzel. *Combined experimental and DFT-TDDFT computational study of photoelectrochemical cell ruthenium sensitizers*, J. Am. Chem. Soc. **2005** 127(48), 16835-16847

[8] Jianjun He, Gabor Benkö. Ferenc Korodi, Tomás Polivka, Reiner Lomoth, Björn Äkermark, Licheng Sun, Anders Hagfeldt, Villy Sundström, *Modified Phthalocyanines for Efficient Near-IR Sensitization of Nanostructured* TiO_2 *Electrode*, J. Am. Chem. Soc. **2012** 124(17), 4922-4932

[9] Paidi Yella Reddy, Lingamallu Giribabu, Christopher Lyness, Henry J. Snaith, Challuri Vijaykumar, Malapaka Chandrasekharam, Mannepalli Lakshmihantam, Jun-Ho Yum, Kuppuswamy Kalyanasundaram, Michael Grätzel, Mohammad K. Nazeeruddin. *Efficient Sensitization of Nanocrystalline TiO2 Films by a Near-IR-Absorbing Unsymmetrical Zinc Phthalocyanine*, Angewandte Chemie International Edition **2007** 46(3), 373-376

[10] Joanna Wiberg, Tannia Marinado, Daniel P. Hagberg, Licheng Sun, Anders Hagfeldt, Bo Albinsson. *Effect of Anchoring Group on Electron Injection and Recombination Dynamics in Organic Dye-Sensitized Solar Cells*, J. Phys. Chem. C **2009** 113, 3381-3886

[11] Ching-Yao Lin, Chen-Fu Lo, Liyang Luo, Hsueh-Pei Lu, Chen-Shiung Hung, Eric Wei-Guang Diau. *Design and Characterization of Novel Porphyrins with Oligo(phenylethylnl) Links of Varied Length for Dye-Sensitized Solar Cells: Synthesis and Optical, Electrochemical, and Photovoltaic Investigation*, J. Phys. Chem. C **2009** 113,

755-764

[12] Crustina Cornaro, Angelo Andreotti. *Solar spectral irradiance measurements relevant to photovoltaic applications*, Proceedings of the III International Conference on Applied Energy **2011** 97

[13] Mohammad K. Nazeeruddin, Robin Humphry-Baker, Michael Grätzel, Dieter Wöhrle, Günter Schnurpfeil, Gerhard Schneider, Andreas Hirth, Nicola Trombach. *Efficient near-IR sensitization of nano crystalline* TiO_2 *films by zinc and aluminium phthalocyanines*, Porphyrins Phthalocyanines **1999** 3(3), 230-237

[14] Grep Kopp, Judith L. Lean, *A new, lower value of total solar irradiance: Evidence and climate significance*, Geophysical Research Letters **2011** 38(1) L01706

[15] The Photophysics behind Photovoltaics and Photonics, Prof. Guglielmo Lanzani 2012 Wiley-VCH

[16] Solar cells for cheap. A MIT Technology Review interview with Prof. M. Grätzel by Kevin Bullis, September 12, 2006
http://www.technologyreview.com/news/406500/solar-cells-for-cheap/

[17] Martin A. Green, Keith Emery, Yoshihiro Hishikawa, Wilhelm Warta Ewan D. Dunlop. *Solar cell efficiency table (version 41)*, Progress in Photovoltaics: Research and Application **2013** 21(1), 1-11

[18] Erik Göransson. *Brigde Mediated Electron Transfer in conjugated and Cross-Conjugated Donor Acceptor Compounds*, ISBN 978-91-554-8474-3

[19] Walter R. Duncan and Oleg V.Prezhdo, *Theoretical Studies of Photoinduced Electron Transfer in Dye-Sensitized* TiO_2, Annu. Rev. Phys. Chem. **2007** 58:143-84

[20] Chuan-Pei Lee, Po-Yen Chen, R.Vittal, Kuo-Chuan Ho. *Iodine-free high efficient quasi solid-state dye-sensitized solar cell containing ionic liquid and polyaniline-loaded carbon black*, J. Mater. Chem. **2010** 20, 2356-2361

[21] C. Ruckebusch, M.Sliwa, P.Pernot, A. de Juan, R. Tauler, *Comprehensive data analysis of femtosecond transient absorption spectra: A review*, Journal of Photochemistry and Photobiology C: Photochemistry Reviews **2012** 13, 1-27

[22] Monishka Rita Narayan. *Review: Dye sensitized solar cells based on natural* photosensitizers, Renewable and Sustainable Energy Reviews **2012** 16. 208-215

[23] Tebello Nyokong, Zbigniew Gasyna, Martin J. Stillman. *Phthalocyanine π-Cation-Radical Species: Photochemical and Electrochemical Preparation of* $[ZnPc(-1)]^{\cdot +}$ Inorg. Chem. **1987** 26, 548-553

[24] Janne Savolainen, *Coherent Controlof Biomolecules*, **2008**, ISBN 978-90-365-2671-5

[25] P. Charlesworth, T.G. Truscott, R.C. Brooks, B.C. Wilson. *The photophysical properties of a ruthenium-substituted phthalocyanine* Journal of Photochemistry and Photobiology B: Biology **1994** 26, 277-282

[26] http://www.chemphys.lu.se/research/projects/wholedssc/

[27] http://www.newport.com/Introduction-to-Solar-Radiation/411919/1033/content.aspx

[28] http://www.green-blog.org/2010/03/09/solar-power-will-take-over-soon/

[29] http://www.rp-photonics.com/prism_pairs.html

Appendices

A. Schematics of electronics for dynamic sample holder

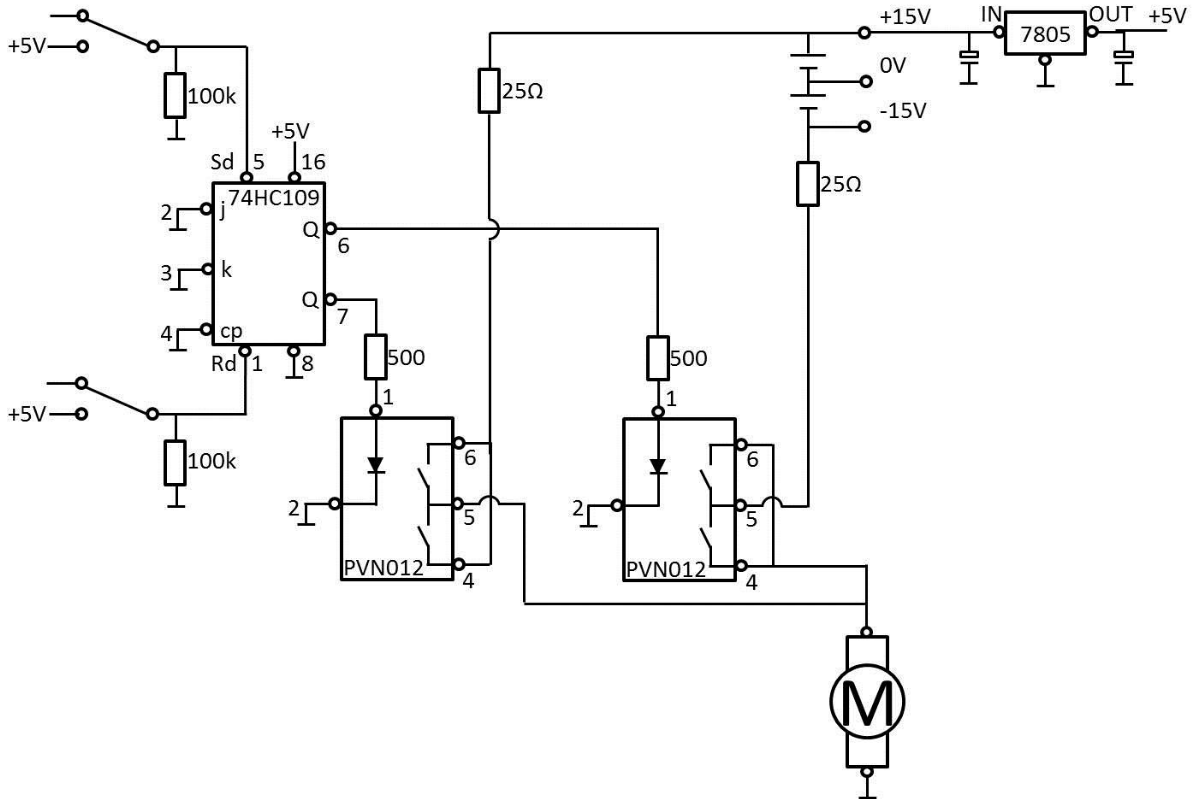

Figure A.1 – Electronic scheme.

B. Beam size of pump and probe

In order to measure the beam size of the probe and pump, a CCD camera was set up at the focus point of the probe beam. To avoid destroying the CCD camera several NDFs had been set in the paths of the pump and the probe beams.

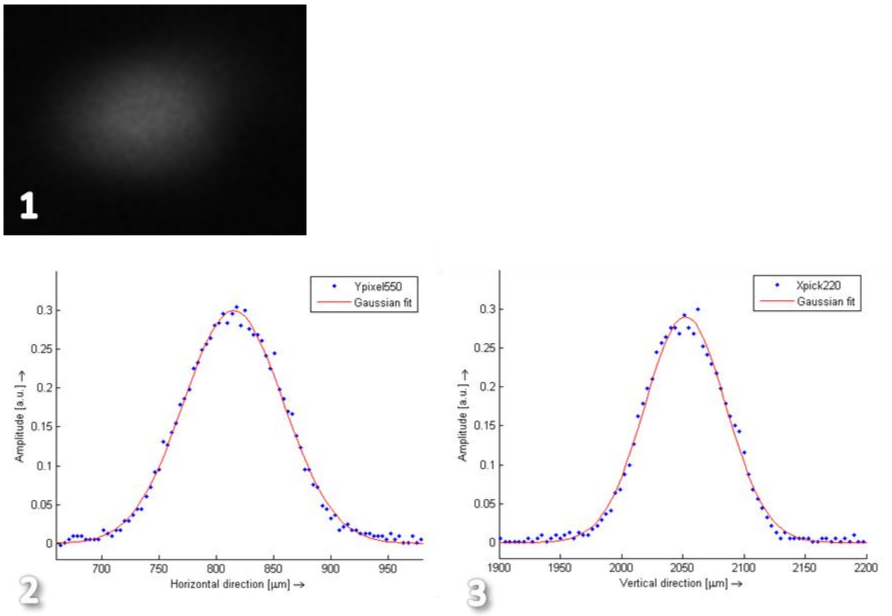

Figure B.1 – (1) image of pump the CCD camera. (2) horizontal profile pump beam 0.299*exp(-((x-815)/61.8)^2) , corresponding to 102 µm. . (3) vertical profile pump beam 0.290*exp(-((x-2052)/46.9)^2) , corresponding to 78 µm.

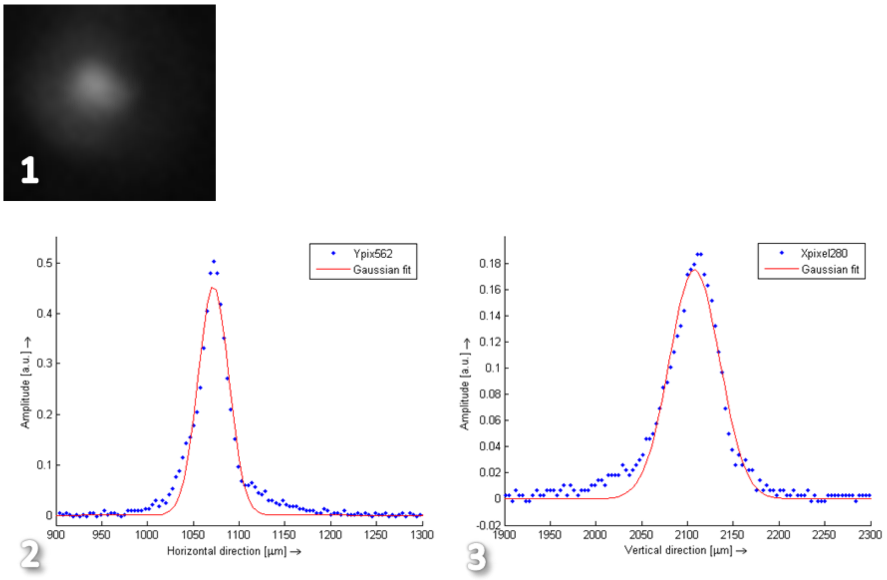

Figure B.2 – (1) image of probe the CCD camera. (2) horizontal profile probe beam 0.454*exp(-((x-1072)/23.6)^2), corresponding to 39 µm. (3) vertical profile probe beam 0.175*exp(-((x-2108)/38.9)^2), corresponding to 65 µm.

C. Pulse duration

Time duration measurements on the pump pulses have been performed by the SGH autocorrelator described in paragraph 3.3. Using the direct feedback of the SGH-autocorrelator the pulses were compressed to near Fourier transform limited pulses. The Labview program offers the option to average the data. In Figure C.1 the normalised and three times averaged signal is shown. From the Gaussian fit a pulse time duration is extracted of 22.7 ± 0.2 fs . By adding a 2 mm NDF this time duration became 25.7 ± 0.2fs.

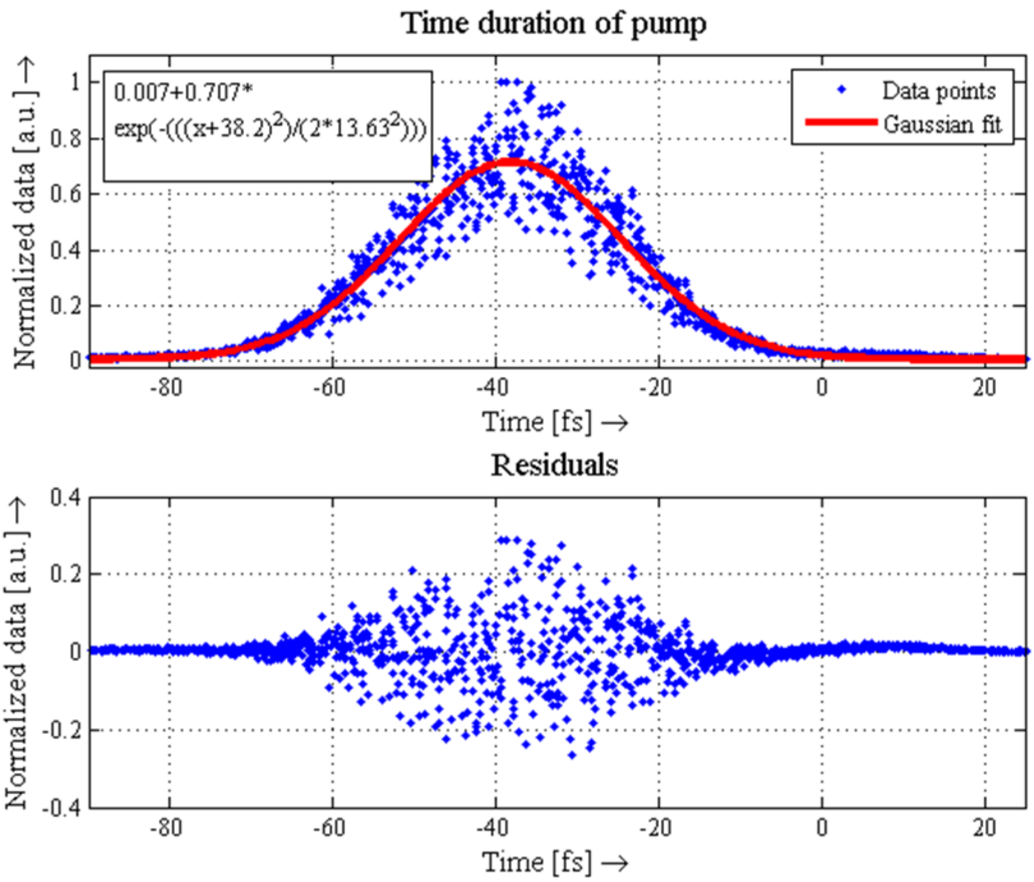

Figure C.1 – Gauss fit on autocorrelation data.

D. Chirp characterisation

A peak can be observed at 513 nm at times 0.40-0.45 ps. This peak has a very small bandwidth, evolves shortly after the time zero delay and the event is very short in time. Moreover by analysing the transient absorption measurement done on a 2 mm glass slide, which had been done for chirp correction (see Figure D.1), the same events can be seen. Therefore I think this event and the event evolving at 0.8 ps -0.9ps (~583 nm) are coherent artefacts.[21]

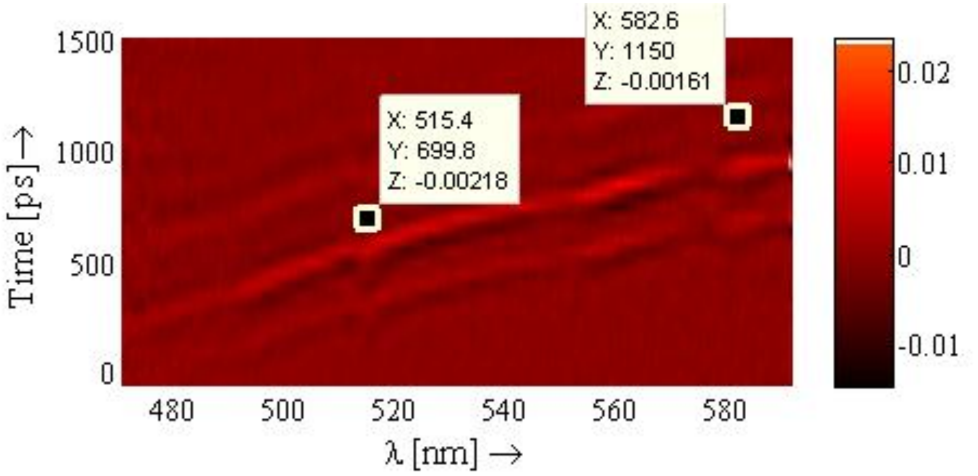

Figure D.1 – 2d plot of transient absorption done on a 2 mm tick glass slide, recorded for chirp characterisation in the 500 nm regime.

The system exhibits a chirp (in wavelength regime 471-594 nm) of 6.23 $\mathrm{fs \cdot nm^{-1}}$ primarily due to the lenses used in the probe path.

E. 2d data plots of TT6, TT7 and TT15

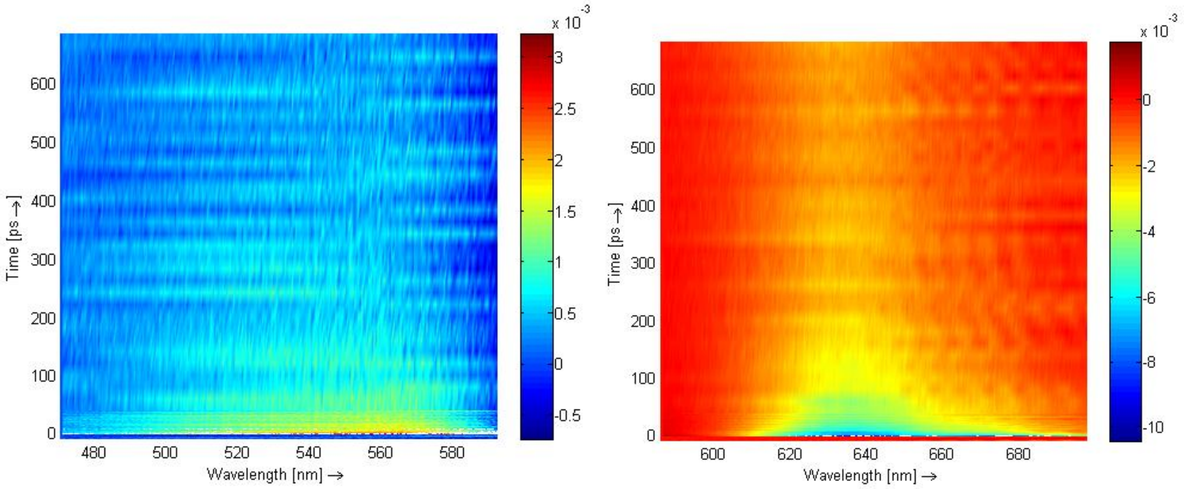

Figure E.1 – TT6-TiO2 (471-592 nm and 586-698 nm)

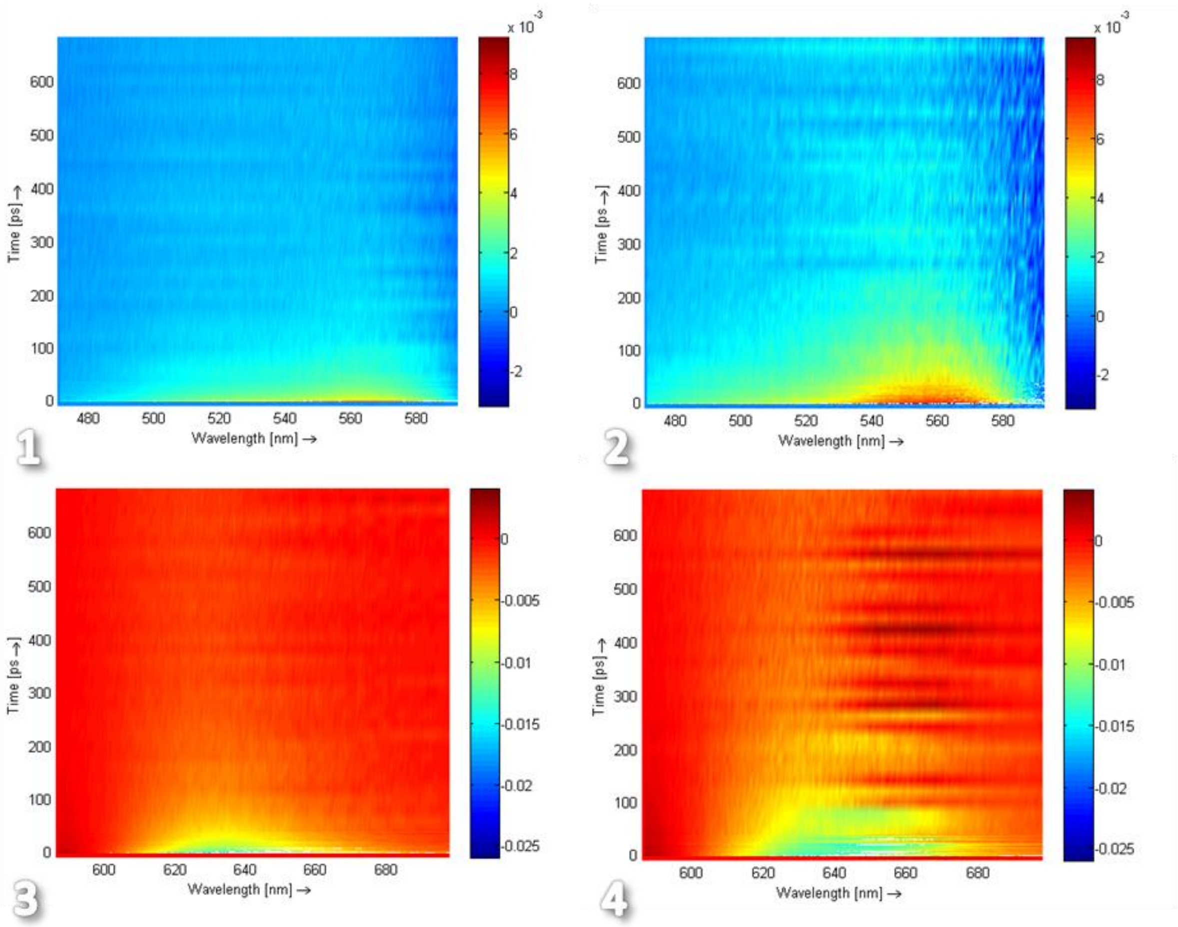

Figure E.2 – TT7-TiO2 (1, 3) and TT7-Al_2O_3 (2, 4)

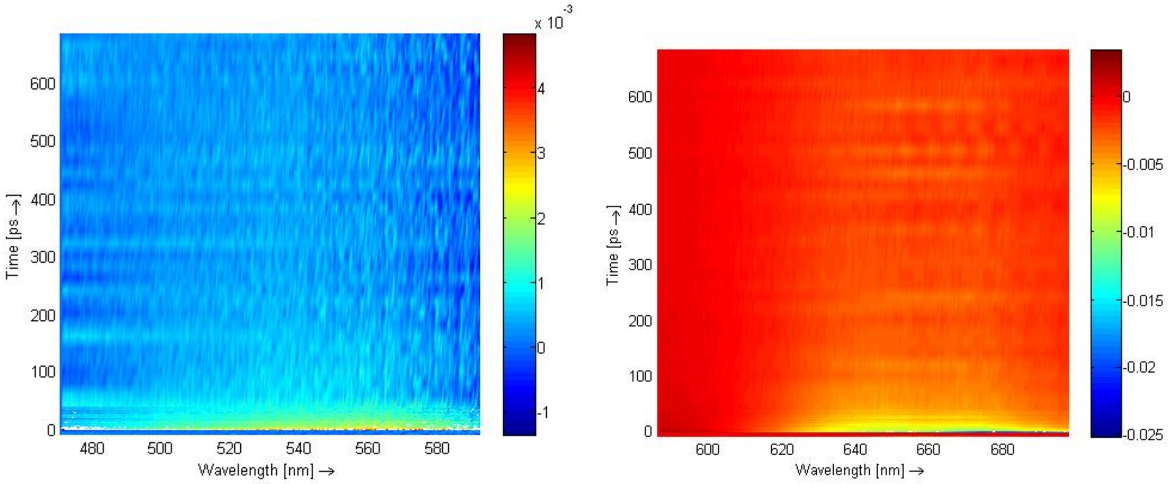

Figure E.3 –2d plot: transient absorption TT15-TiO_2 film. Lambda 510